AD_____

GRANT NO: DAMD17-94-J-4368

TITLE: pH Regulation by Breast Cancer Cells In Vitro and In Vivo.

PRINCIPAL INVESTIGATOR: Robert J. Gillies, Ph.D

CONTRACTING ORGANIZATION: University of Arizona
Tucson, AZ 85719

REPORT DATE: September 29, 1995

TYPE OF REPORT: Annual Report

PREPARED FOR: U.S. Army Medical Research and Materiel Command
Fort Detrick, Maryland 21702-5012

DISTRIBUTION STATEMENT: Approved for public release; distribution unlimited

REPORT DOCUMENTATION PAGE

Form Approved
OMB No. 0704-0188

1. AGENCY USE ONLY (Leave blank)	2. REPORT DATE	3. REPORT TYPE AND DATES COVERED
	29 Sep 1995	15 Aug 94 - 14 Aug 95 Annual

4. TITLE AND SUBTITLE
pH Regulation by Breast Cancer Cells In Vitro and In Vivo

5. FUNDING NUMBERS
DAMD17-94-J-4368

6. AUTHOR(S)
Robert J. Gillies, Ph.D.

7. PERFORMING ORGANIZATION NAME(S) AND ADDRESS(ES)
University of Arizona
Tucson, Arizona 85719

8. PERFORMING ORGANIZATION REPORT NUMBER

9. SPONSORING/MONITORING AGENCY NAME(S) AND ADDRESS(ES)
U.S. Army Medical Research and Materiel Command
Fort Detrick, Maryland 21702-5012

10. SPONSORING/MONITORING AGENCY REPORT NUMBER

11. SUPPLEMENTARY NOTES

12a. DISTRIBUTION/AVAILABILITY STATEMENT
Approved for public release; distribution unlimited

12b. DISTRIBUTION CODE

13. ABSTRACT *(Maximum 200 words)*

pH is a fundamental parameter of tumor progression. We are investigating the mechanisms regulating both the intracellular and extracellular pH of breast cancer tumors, both *in vivo* and *in vitro*. For extracellular pH studies, we are using ^{31}P-NMR spectroscopy of human breast cancer tumors grown in nude mice. In these studies, extracellular pH is measured using an exogenous compound, 3-aminopropylphosphonate (3-APP), and intracellular pH is measured using endogenous inorganic phosphate. Over the past year, we have been refining these techniques, which are now in use by at least three other labs in the world. For measurement of intracellular pH, we are using fluorescence spectroscopy and molecular biological techniques to characterize the activity of plasma membrane associated Vacuolar type H^+-ATPase (pV-ATPase). This pump is highly active in approximately half of the tumor cell lines investigated, and correlates highly with both invasive potential and drug resistance. We hypothesize that these are related and can be explained by a rapid rate of endomembrane recycling.

14. SUBJECT TERMS
pH, NMR Spectroscopy, Multidrug Resistance, Vacuolar-type ATPases, Invasion, Endosomal Recycling.
breast cancer

15. NUMBER OF PAGES
50

17. SECURITY CLASSIFICATION OF REPORT	18. SECURITY CLASSIFICATION OF THIS PAGE	19. SECURITY CLASSIFICATION OF ABSTRACT	20. LIMITATION OF ABSTRACT
Unclassified	Unclassified	Unclassified	Unlimited

GENERAL INSTRUCTIONS FOR COMPLETING SF 298

The Report Documentation Page (RDP) is used in announcing and cataloging reports. It is important that this information be consistent with the rest of the report, particularly the cover and title page. Instructions for filling in each block of the form follow. It is important to ***stay within the lines*** to meet ***optical scanning requirements***.

Block 1. Agency Use Only *(Leave blank)*.

Block 2. Report Date. Full publication date including day, month, and year, if available (e.g. 1 Jan 88). Must cite at least the year.

Block 3. Type of Report and Dates Covered. State whether report is interim, final, etc. If applicable, enter inclusive report dates (e.g. 10 Jun 87 - 30 Jun 88).

Block 4. Title and Subtitle. A title is taken from the part of the report that provides the most meaningful and complete information. When a report is prepared in more than one volume, repeat the primary title, add volume number, and include subtitle for the specific volume. On classified documents enter the title classification in parentheses.

Block 5. Funding Numbers. To include contract and grant numbers; may include program element number(s), project number(s), task number(s), and work unit number(s). Use the following labels:

C	- Contract	**PR**	- Project
G	- Grant	**TA**	- Task
PE	- Program Element	**WU**	- Work Unit Accession No.

Block 6. Author(s). Name(s) of person(s) responsible for writing the report, performing the research, or credited with the content of the report. If editor or compiler, this should follow the name(s).

Block 7. Performing Organization Name(s) and Address(es). Self-explanatory.

Block 8. Performing Organization Report Number. Enter the unique alphanumeric report number(s) assigned by the organization performing the report.

Block 9. Sponsoring/Monitoring Agency Name(s) and Address(es). Self-explanatory.

Block 10. Sponsoring/Monitoring Agency Report Number. *(If known)*

Block 11. Supplementary Notes. Enter information not included elsewhere such as: Prepared in cooperation with...; Trans. of...; To be published in.... When a report is revised, include a statement whether the new report supersedes or supplements the older report.

Block 12a. Distribution/Availability Statement. Denotes public availability or limitations. Cite any availability to the public. Enter additional limitations or special markings in all capitals (e.g. NOFORN, REL, ITAR).

- **DOD** - See DoDD 5230.24, "Distribution Statements on Technical Documents."
- **DOE** - See authorities.
- **NASA** - See Handbook NHB 2200.2.
- **NTIS** - Leave blank.

Block 12b. Distribution Code.

- **DOD** - Leave blank.
- **DOE** - Enter DOE distribution categories from the Standard Distribution for Unclassified Scientific and Technical Reports.
- **NASA** - Leave blank.
- **NTIS** - Leave blank.

Block 13. Abstract. Include a brief *(Maximum 200 words)* factual summary of the most significant information contained in the report.

Block 14. Subject Terms. Keywords or phrases identifying major subjects in the report.

Block 15. Number of Pages. Enter the total number of pages.

Block 16. Price Code. Enter appropriate price code *(NTIS only)*.

Blocks 17. - 19. Security Classifications. Self-explanatory. Enter U.S. Security Classification in accordance with U.S. Security Regulations (i.e., UNCLASSIFIED). If form contains classified information, stamp classification on the top and bottom of the page.

Block 20. Limitation of Abstract. This block must be completed to assign a limitation to the abstract. Enter either UL (unlimited) or SAR (same as report). An entry in this block is necessary if the abstract is to be limited. If blank, the abstract is assumed to be unlimited.

FOREWORD

Opinions, interpretations, conclusions and recommendations are those of the author and are not necessarily endorsed by the US Army.

Where copyrighted material is quoted, permission has been obtained to use such material.

Where material from documents designated for limited distribution is quoted, permission has been obtained to use the material.

Citations of commercial organizations and trade names in this report do not constitute an official Department of Army endorsement or approval of the products or services of these organizations.

In conducting research using animals, the investigator(s) adhered to the "Guide for the Care and Use of Laboratory Animals," prepared by the Committee on Care and Use of Laboratory Animals of the Institute of Laboratory Resources, National Research Council (NIH Publication No. 86-23, Revised 1985).

For the protection of human subjects, the investigator(s) adhered to policies of applicable Federal Law 45 CFR 46.

In conducting research utilizing recombinant DNA technology, the investigator(s) adhered to current guidelines promulgated by the National Institutes of Health.

In the conduct of research utilizing recombinant DNA, the investigator(s) adhered to the NIH Guidelines for Research Involving Recombinant DNA Molecules.

In the conduct of research involving hazardous organisms, the investigator(s) adhered to the CDC-NIH Guide for Biosafety in Microbiological and Biomedical Laboratories.

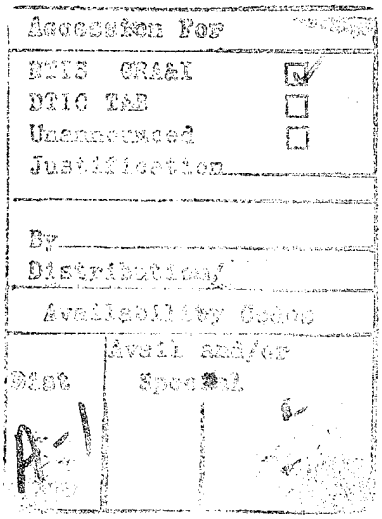

SEP. 29, 1995

PI - Signature Date

Initialed & signed by:
Natarajan Raghunand, Ph.D,
for Robert J. Gillies, Ph.D (PI)

Table of Contents

INTRODUCTION

The pH of tumors, both intracellular and extracellular, is a fundamental parameter of cancer progression. All available evidence indicates that the extracellular pH (pH_{ex})of tumors is acidic, while the intracellular pH (pH_{in}) is relatively alkaline (Griffiths et al., 1991). An acidic extracellular pH is clastogenic (Morita et al., 1992) and can induce tumorigenic transformation (LeBoeuf et al., 1990) and a metastatic phenotype (Schlappack et al., 1993). An alkaline intracellular pH is required for cell proliferation (Gillies and Martinez-Zaguilan, 1991).

During the past year, we have been refining methods to non-invasively measure intra- and extracellular pH of tumors *in vivo*, using ^{31}P-NMR spectroscopy. This work has resulted in one published abstract and a manuscript in preparation. We have also been investigating the mechanisms of pH regulation in breast cancer cells, especially the activity of plasma membrane-associated Vacuolar-type H^+-ATPase activity (pV-ATPase). Our results to date are incomplete, but illustrate an emerging correlation between pV-ATPase activity, invasive potential and drug resistance. We believe all of these may be related, if the elevated pV-ATPase activity is an indicator for rapid endomembrane recycling. Endomembrane recycling is involved in both invasive behavior and multidrug resistance. We are investigating these relationships, and have formulated a general model to quantitatively account for the involvement of endomembrane recycling in multidrug resistance. A manuscript is being prepared describing this work, and it is appended.

BODY

1. Measurement of intracellular and extracellular pH of tumors *in vivo*.

We have continued our efforts to refine methods for the non-invasive measurement of intra- and extracellular pH of tumors *in vivo*. Extracellular pH is measured by the ^{31}P-NMR resonance of 3-aminopropylphosphonate (3-APP) while intracellular pH is measured simultaneously by the ^{31}P-NMR resonance of inorganic phosphate. The major advancements of the last year have been the generation of a robust titration curve for 3-APP, and the development of techniques to deconvolve the effects of magnetic field heterogeneity and pH heterogeneity on the lineshape of the 3-APP resonance. The deconvolved spectrum can then be used to generate a true extracellular pH profile for individual tumors. The methods we have developed have been applied by groups at Johns Hopkins University School of Medicine, St. George's Hospital Medical School in London, and at the Skeyby University Hospital in Aarhus, Denmark. Results have been published as full papers (McCoy et al., 1995) as well as abstracts (Gillies et al, 1995; Maxwell et al, 1995). These results uniformly show that the extracellular pH of tumors is lower than that of normal tissue, and that the extracellular pH of large tumors is lower than that of small tumors.

We have also begun work on an extracellular pH indicator visible by ^{1}H-NMR spectroscopy. The advantage of this indicator is that it will be amenable to imaging, allowing us to determine the localized pH within tumors.

Following is a complete description of our activities under this sub-project during the past year.

Measurement of the true distribution of extracellular pH within tumors. A good NMR-visible *in vivo* pH_{ex} indicator should possess the following properties:

- It should be non-cytotoxic at high concentrations in the blood (to maximize the signal-to-noise ratio in the NMR spectrum)
- It should be impermeable to the plasma membrane (so that the indicator does not respond to pH_{in})
- It should have a pK_a near neutrality (to give the indicator maximum sensitivity in the physiological range)
- Its resonance should be well resolved from other peaks in the spectrum
- There should be a large change in chemical shift between the titration end-points (to increase precision of the pH measurement)

3-aminopropylphosphonate has been established to be non-cytotoxic to C6 glioma and Ehrlich Ascites Tumor cells (Gillies et al., 1994), and to MCF-7 cells (Gillies et al., 1995). In addition, it does not cross the plasma membrane of cells, and its position on a typical *in vivo* ^{31}P-NMR spectrum assures non-interference by other peaks. For 3-APP to be useful as an *in vivo* pH indicator, its chemical shift must be dependent only on the hydrogen ion concentration in its environment, and must be independent of other environmental factors such as the concentrations of other cations and anions. Titrations of the chemical shift of 3-APP against pH performed in our laboratory agreed closely with those performed elsewhere, despite differences in buffer composition and spectrometer hardware (fig. 1).

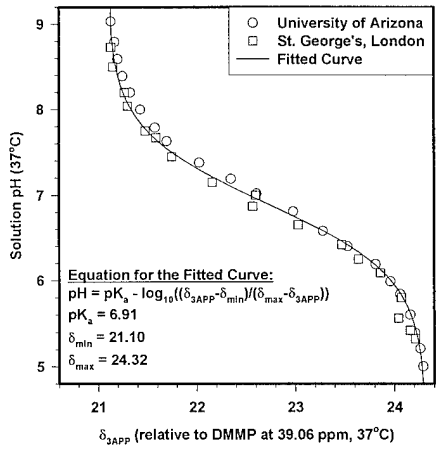

Figure 1. ^{31}P-NMR Titration Curves for 3-APP obtained by us, and at St. George's Hospital Medical School, London. The titrations were performed at 37°C, and chemical shifts are referenced to dimethyl methylphosphonate (DMMP).

There are many potential sources of error when determining pH from the chemical shift of a compound (Madden et al., 1991):

- Assignment of chemical shift in the absence of a reference *in vivo*. In the case of 3-APP, errors in referencing on the downfield side will lower the apparent pH_{in}, and errors on the upfield side will have the opposite effect. Our strategy has been to reference *in vivo* spectra to the α-NTP peak at -10.05 ppm and Phosphocreatine at -2.54 ppm. Spectra in which the chemical shift difference between these two peaks is significantly different from 7.51 ppm are discarded. Alternately, dimethyl methylphosphonate (DMMP) injected into the animals prior to acquiring the spectra can be used as a good *in vivo* chemical shift reference.
- Peak overlap. In the case of 3-APP, this is not a problem, since the resonance of 3-APP is very well resolved from other species.
- Poor signal-to-noise. This has been overcome by increasing the dosage of 3-APP given to the animal (McCoy et al, Br. J. Can. 1995).
- B_0-inhomogeneity induced broadening of the 3-APP peak.

This last point deserves special attention. The 3-APP peak in an *in vivo* ^{31}P-NMR spectrum has a finite spread which arises not just from the pH heterogeneity within the tumor sample, but also due to transverse relaxation (T_2) effects, and inhomogeneities in the magnetic field strength within the sample volume. The latter two effects may be combined into one, a T_2* effect. In the absence of any T_2* effects, the chemical shift corresponding to each point on a 3-APP peak from a volume-averaged ^{31}P-NMR spectrum of a tumor would represent a distinct pH, and the intensity of the peak at each pH point would be roughly related to the fraction of the vascular volume in the tumor at that pH.

However, in the presence of T_2* effects, the observed 3-APP peak is a convolution of two peaks --- one representing only the pH heterogeneity within the tumor, and the other representing the T_2* effects. To deconvolve the two peaks, one needs 1) the 3-APP resonance in a ^{31}P-NMR spectrum of a tumor, and, 2) another spectrum obtained under identical conditions from the same tumor in which the broadening of the 3-APP peak results only from heterogeneities in the magnetic field within the tumor and transverse relaxation by 3-APP molecules within the tumor, but not any pH heterogeneities within the tumor. We have sought to approximate the T_2* effects by the lineshape of the 3-APP resonance in spectra from tumors following sacrifice of the animal. The rationale behind these experiments is that following death, the extracellular pH within the tumor should gradually approach uniformity, while heterogeneities in the magnetic field should persist. The lack of pH heterogeneity in tumors within 30-60 minutes of death was verified by us by ^{1}H-Chemical Shift Imaging using pH-sensitive imidazole compounds (see page 6 of this progress report). For the deconvolution to yield meaningful results, the magnetic field heterogeneities within the tumor following sacrifice should be identical to those prevalent in the living animal. The sacrifice can be achieved without moving the animal within the magnet, thus keeping gross alterations in the magnetic field heterogeneities within the

tumor to a minimum. Some concerns remain that the lack of blood flow in the tumor following death, and alterations in the oxidative state of the hemoglobin in the tumor blood stream following death will alter the magnetic microenvironment and relaxation properties of 3-APP molecules within the tumor. These would tend to broaden the 3-APP resonance, making our deconvolved data represent the lower limit of the pH distribution. In the future, we will obtain ^{1}H-NMR spectra of the water resonance before and after death to correct for these effects. We also expect to relate the T_2^* to resonances available in the living animals, which will allow us to correct for this parameter without sacrificing the animals. The mathematical principles underlying the deconvolution technique are now explained.

Convolution Theorem. The Fourier transform of a convolution of two functions is proportional to the products of their individual Fourier transforms. Conversely, the Fourier transform of a product of two functions is proportional to the convolution of their individual Fourier transforms.

NMR experiments yield data in the form of "Free Induction Decays" (FIDs), which consist of signals with intensities varying periodically in the time domain, while undergoing exponential decay. Fourier transformation of the FIDs yield the familiar NMR spectra in the frequency domain. The Convolution Theorem stated above offers us the ability to deal with a convolution of two functions in the frequency domain as simple multiplications in the time domain. Thus, if the Fourier transforms of two functions --- say, f_{T2^*} and f_{pH} --- are convolved (in the frequency domain), such that:

$$F_o(\nu) = F_{T2^*}(\nu) \otimes F_{pH}(\nu); \qquad (\text{"}\otimes\text{" represents the convolution operation})$$

then, in the time domain, we have:

$$f_o(t) = f_{T2^*}(t) \bullet f_{pH}(t); \qquad (\text{"}\bullet\text{" represents a scalar multiplication})$$

Here, upper case functions are Fourier transforms of corresponding lower case functions. Thus, lower case functions are FIDs in the time (t) domain, and upper case functions are spectra in the frequency (ν) domain.

In our case, $F_o(\nu)$ is the 3-APP region of the ^{31}P-NMR spectrum obtained from a tumor in the live animal, and $F_{T2^*}(\nu)$ is the 3-APP region of the ^{31}P-NMR spectrum obtained from the same tumor following death of the animal. Inverse Fourier transformation of $F_o(\nu)$ yields $f_o(t)$, and inverse Fourier transformation of $F_{T2^*}(\nu)$ yields $f_{T2^*}(t)$.

Thus, $f_{pH}(t)$, the FID corresponding to a 3-APP resonance containing information on only the pH heterogeneity within the tumor may be obtained as follows:

$$f_{pH}(t) = f_o(t)/f_{T2^*}(t)$$

Fourier transformation of $f_{pH}(t)$ yields the desired spectrum, $F_{pH}(\nu)$, the width of the 3-APP peak in which contains information about only pH heterogeneity within the tumor.

Treatment of Noise in the Spectra. The presence of noise in NMR spectra complicates the analysis presented above, and the deconvolution of a "noisy" spectrum from another spectrum requires the use of filters to enhance the quality of the output. For our case, where the noise is additive and where the intensity of the noise is independent of its frequency, a Wiener filter is the optimum filter (Blinchikoff and Zverev, 1986). The appropriate Wiener filter was estimated using a FORTRAN routine provided by Taylor and Smith (Taylor and Smith, 1976) and applied to the deconvolved FID ($f_{pH}(t)$, in the example above).

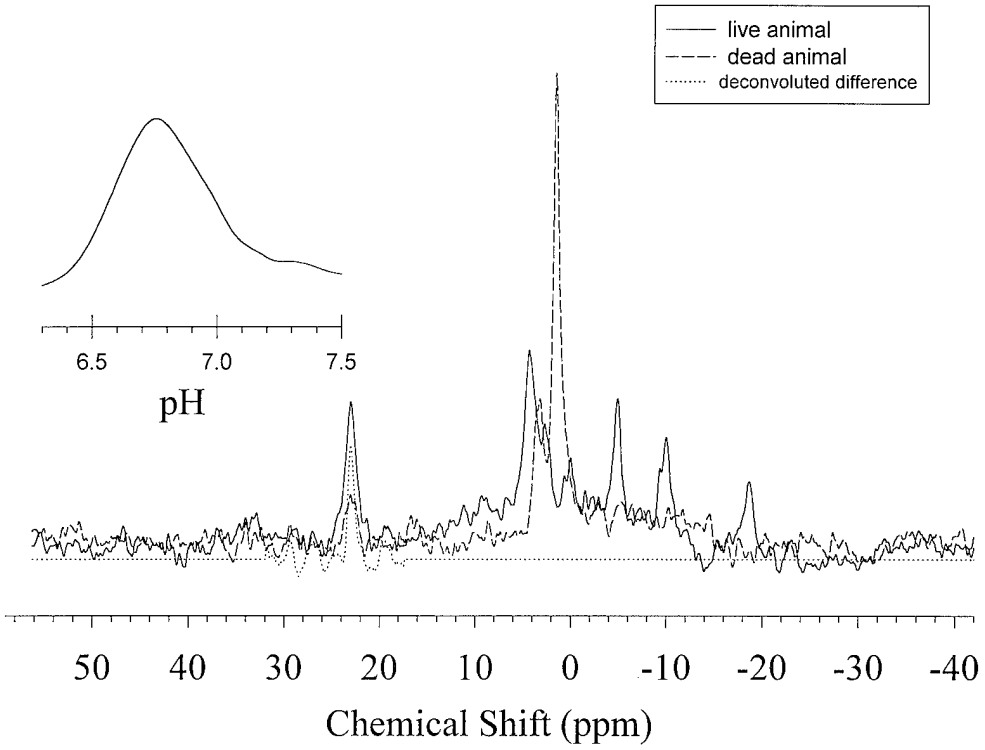

Figure 2. Deconvolution of T_2^* effects from pH heterogeneity effects from the 3-APP resonance in ^{31}P-NMR spectra from CaNT tumors grown in CBA/Gy fTO mice. Inset shows the pH_{ex} distribution within the tumor corresponding to the deconvolved 3-APP peak.

Deconvolution of *in vivo* spectra. Figure 2 shows the results of the deconvolution of the 3-APP region of a ^{31}P-NMR spectrum of a CaNT tumor grown subcutaneously on the lower dorsum of synergic CBA/Gy fTO mice (McCoy et al., 1995). Spectra of tumors, both before and after sacrifice of the animals were provided to us by Dr. Marion Stubbs at St. George's Hospital Medical School in London. The deconvolution was carried out on the 3-APP

regions of spectra from the live and dead animals as outlined above. The chemical shift of each point on the deconvolved 3-APP peak was then converted to an equivalent pH value using the titration curve and equation shown in figure 1.

Chemical Shift Imaging (CSI). In addition to the technique presented so far, another option for investigating the pH profile of tumors exists. In 3-D chemical shift imaging, NMR spectra are obtained from all points within the region of interest, and an image can be extracted from any or all resonance frequencies, allowing images of particular chemical moieties to be presented (Brink et al., 1989). If the resonance frequency chosen to form the images is one of a pH-sensitive nucleus, then it is possible to construct a 3-D "pH-map" of a sample, such as a tumor. While 3-APP allows us to obtain information on the extracellular pH profile of tumors as explained so far, the ^{31}P nucleus provides an inherently weaker NMR response than the ^{1}H nucleus. As such, the time required to obtain the pH-map is substantially longer when one deals with a pH-probe which is ^{31}P-NMR-visible, as opposed to one which is ^{1}H-NMR-visible.

Imidazol-1-ylalkanoic acids as ^{1}H-NMR pH probes. The ^{1}H spectrum covers a smaller range of frequencies than the ^{31}P spectrum, for a given magnet strength. This potentially reduces the precision of the pH measurement made by ^{1}H-NMR spectroscopy as compared to ^{31}P-NMR spectroscopy. However, the greater signal strength from ^{1}H nuclei will facilitate a 3-dimensional mapping of the pH_{ex} distribution in a tumor by Chemical Shift Imaging. Cerdan and Ballesteros (Gil et al., 1994; Zaderenko et al., 1994) have developed a family of imidazole compounds which have shown promise as extrinsic *in vivo* pH probes. After testing the compounds for cytotoxicity, we have narrowed down our choices to two: diethyl 2-pyrazol-1-ylsuccinate and 3-(ethoxycarbonyl)-2-benzimidazol-1ylpropionic acid. We have carried out titrations of these two compounds (fig. 3) and have begun utilizing them for *in vivo* chemical shift imaging. In our early attempts at obtaining CSI images of tumors grown in mice, we have found that these compounds leave the animals' blood stream via the kidneys too rapidly to permit good quality images. We are working on solutions to this temporary setback.

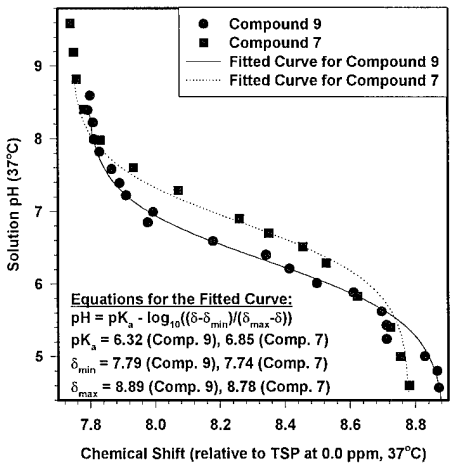

Figure 3. ^{1}H-NMR titration curves of imidazole compounds in fetal bovine serum at 37°C. "Compound 7" refers to Diethyl 2-pyrazol-1-ylsuccinate, and "Compound 9" refers to 3-(Ethoxycarbonyl)-2-benzimidazol-1-ylpropionic acid. (Gil et al., 1994; Zaderenko et al., 1994)

2. Vacuolar type H^+-ATPase activity in breast cancer cells.

According to our hypothesis, highly invasive breast cancer cells will exhibit plasma membrane-associated vacuolar-type H^+-ATPase activity (pV-ATPase) while non-invasive cell lines will not. In accordance with our stated objectives, the cell lines employed in this study were non-invasive MCF-7 and MDA-MB-468, and the highly invasive MDA-MB-231 and MDA-MB-435. We have also added some new cell lines to this study, representing drug-resistant variants of MCF-7 cells, as well as a spontaneously immortalized breast epithelial line, MCF-10 (Soule et al., 1990) along with its transfected variants. MCF-10neo were transfected with neomycin resistance plasmid, MCF-10neoN were transfected with a plasmid containing the human Ha-ras protooncogene, and MCF-10neoT were transfected with a plasmid containing human Ha-ras oncogene with a T-24 mutation (Basolo et al., 1991). The MCF-10neoT cells are highly invasive in *in vitro* assays, while the other cell lines are not (Miller et al., 1993).

While our studies are not yet complete, the following table illustrates our results to date using these cells.

Table 1. Relationship between metastatic potential and expression of pV-ATPase activity. "-" = very low; "+" = high; "n.d" = not determined

Cell Line	Metastasis	pH_{in} (at pH_{ex} 7.15)	pV-ATPase
MCF-7-S	-	7.1 +/- 0.1	NO
MCF-7-MITOX	n.d	7.2 +/- 0.1	YES
MCF-7-DOX	n.d	6.96 +/- 0.2	YES
MDA-MB 435	+++	n.d	YES
MDA-MB 231	+++	n.d	YES
MDA-MB 361	++++	n.d	n.d

Note that there is an emerging correlation between invasiveness and pV-ATPase activity. Such a correlation has previously been documented by us in melanoma cell lines (Martinez-Zaguilan et al., 1995). We believe that this pV-ATPase activity represents a transient expression of pumps at the cell surface which is the result of rapid endomembrane turnover. This hypothesis is also supported by the importance of

endosomal/lysosomal proteases in invasion (Lah et al., 1992) and the regulation of lysosomal protease release by pH (Rozhin et al. 1994). Thus, the observed pV-ATPase activity may be a measure of rapid endomembrane recycling to the cell surface.

Note that the drug-resistant MCF-7 cell lines, MCF-7/DOX (containing p-glycoprotein) and MCF-7/Mitox (p-glycoprotein negative), both contain pV-ATPase activity. Because of this, and the potential importance of endosomal recycling in multidrug resistance (Sehested et al., 1987), we have examined whether rapid recycling of endomembrane systems that are acidified by V-ATPase activity have the potential to effect drug resistance.

3. pH and multidrug resistance.

General model. Acquired resistance to chemotherapeutic agents is a major cause of treatment failure in patients with cancer. Overexpression of the drug efflux transporter, the p-glycoprotein, is associated with multidrug resistance in many but not all cases. We have developed a general model which illustrates that there are multiple mechanisms capable of lowering cytosolic concentrations of weak base drugs, thereby reducing the effectiveness of the drug. These mechanisms include: 1) enhanced endosomal efflux involving active transport of the drug into the endosomes, 2) increased endosomal turnover rates, 3) decreased endosomal pH and/or increased cytosolic pH, 4) decreased passive permeability of the protonated drug species across the endosomal membrane, and, 5) decreased membrane potentials across plasma and/or endosomal membranes. All of these mechanisms have been observed in the literature and different cells can employ various combinations of these parameters to effect multi-drug resistance. The model is presented in greater detail in the **appended manuscript** which is still under preparation.

We have used fluorescent markers to try and measure the possible involvement of endosomal recycling in removal of drug from the cytosol of drug-resistant cells.

Extrusion of Coumarin by drug-resistant cells. Coumarin is a fluorescent marker which is membrane-impermeant and can only be taken up by the cells via endocytosis. The dye localizes to acidic compartments in the cell in much the way that weak-base chemotherapeutic drug molecules localize to acidic vesicles in the cell. Therefore, measurement of extrusion rates of coumarin from the cells will give us estimates of the rates of possible extrusion of drug by the cells via exocytosis.

In these experiments, cells grown on coverslips are incubated in the presence of 50 μg/mL coumarin and placed in the fluorometer in a perfused cuvette. The isoexcitation point of coumarin is a wavelength of 370 nm, and monitoring the signal at this wavelength allows us to monitor the amount of dye within the pathlength of the exciting light. The initial drop (first 5 min.) in signal represents primarily the washing out of the coumarin from the cuvette and coverslip, upon starting the perfusion. Only after the initial washout (beginning around 10 min. after the start of the experiment) do we begin to measure the drop in amount of

dye within the cells themselves. The fluorescence intensity data (I_F) for the two sections of the washout curve --- before 5 minutes and beyond 10 minutes --- were separately fitted to equations of the form:

$$I_F = a \cdot e^{-\alpha \cdot t} + b$$

Here, the time constant α provides us a measure of the specific coumarin extrusion rate by the cells. The value of α for timepoints 10 minutes or more after the start of the washout was taken to represent primarily the rate of active extrusion of coumarin by the cells. Figure 4 illustrates some of our results so far: figure 4a depicts the value of α in cells maintained at 18°C, when the endosomal turnover rate is very low, and figure 4b shows the value of α in cells maintained at 37°C. It is clear from the values of α for the data collected 10 minutes and more after the start of the washout, that the drug efflux rate in the drug-sensitive MCF-7/s cells is lower than the drug efflux rates in the drug-resistant MCF-7/Mitox and MCF-7/DOX cells.

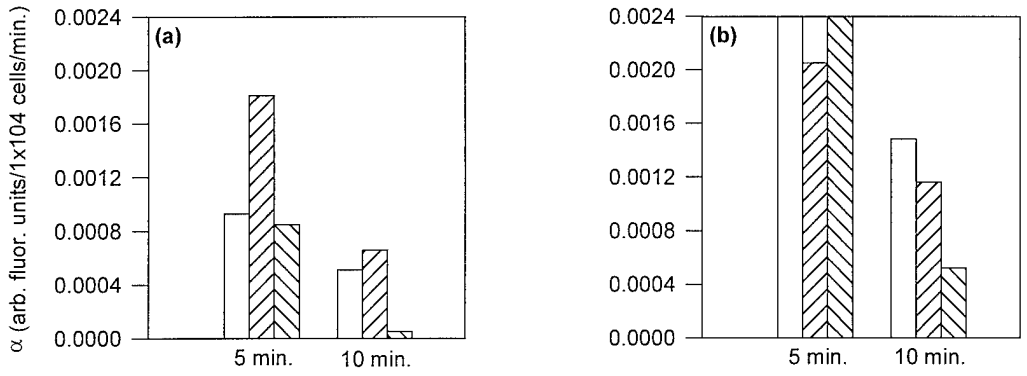

Figure 4. Rates of Coumarin leakage: ☐ MCF-7/MITOX, ▨ MCF-7/Sens., and, ▨ MCF-7/DOX cells. **(a)** cells maintained at 18°C; **(b)** cells maintained at 37°C.

Effect of weak-bases on drug-resistant cells. If sequestration of drug molecules in acidic vesicles is important for drug-resistance, then raising endosomal/lysosomal pH should confer sensitivity. Uptake of weak-bases such as methylamine by acidic vesicles will tend to alkalinize them (Okhuma and Poole, 1978). Drug-resistant MCF-7/DOX cells were grown in the presence of different concentrations of doxorubicin and methylamine. After a 48 hour exposure, the medium was changed to normal growth medium, and the survivability of the cells assayed 72 hours thereafter by glutaraldehyde fixation and vital staining with crystal violet. The effect of methylamine on sensitizing the cells to doxorubicin is shown in figure 5.

Figure 5. Effect of a 48 hour treatment of MCF-7/DOX cells with Doxorubicin and Methylamine.

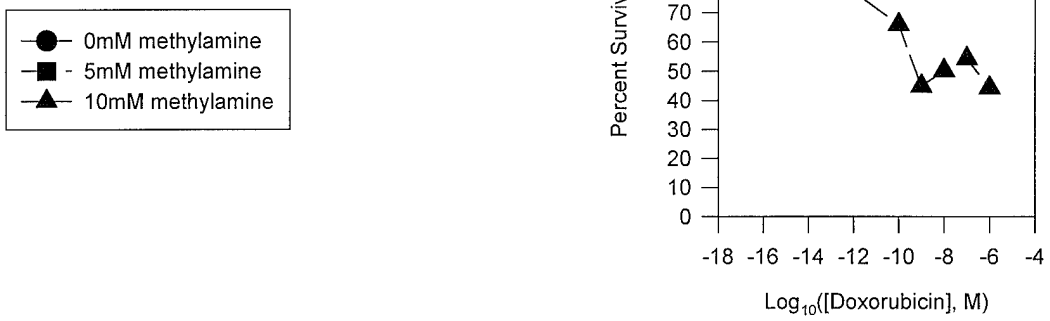

The presence of 10mM methylamine appears to reduce survivability of MCF-7/DOX cells by up to 50% when 1μM doxorubicin is present in the medium, although 0mM and 5mM methylamine had little effect. These are preliminary results, and we wish to be conservative in interpreting these data. We have not yet measured the effect of 10mM methylamine on the endosomal pH gradient in these cells, but from past experience with other cell lines, we would expect 5mM methylamine to raise the pH of endosomes/lysosomes by 0.05-0.1 pH units, while 10mM methylamine would cause a 0.1-0.4 pH unit rise in endosomal pH. The theoretical model presented in the appended manuscript suggests that a rise in endosomal pH of 0.4 pH units would result in a significant rise in the cytoplasmic concentration of the drug at steady state. We are currently engaged in more rigorously investigating the effects of weak bases on the drug-sensitivity of MCF-7/DOX cells.

RELATIONSHIP TO ORIGINAL STATEMENT OF WORK

The studies outlined in the original Statement of Work have been modified somewhat, mostly by the inclusion of additional cell lines. This was justified, since four of these cell lines (the MCF-10 series) represent the pre-cancerous state which, in terms of therapy, is the most important. Thus, the inclusion of these cell lines, while slightly retarding our schedule, is justified. In addition, because of technical reasons, some studies planned for year 01 have been moved to year 02. Consequently, some studies proposed for year 02 are already well underway.

Task 1a, measurement of intracellular and extracellular pH by fluorescence, is well underway and will be completed during this next year. It has been slightly retarded due

to the inclusion of additional cell lines.

Task 1b, measurement of intracellular and extracellular pH of cells grown in bioreactors, has been postponed due to the unavailability of suitable commercial bioreactors. This problem has been rectified, and these studies are being initiated.

Tasks 1c and 1d (data analysis), will be performed following completion of 1b.

Tasks 2a-d, determination of pH regulatory mechanisms, originally scheduled for year 02 are almost complete. The data are all in hand for 4 cell lines and we are currently in a period of data analysis. More studies will be performed as necessary.

Task 3a-d, measurement of pH *in vivo*, has been postponed until this year. Part of this postponement was the unavailability of funds to support the research at Johns Hopkins, where it was performed previously. Thus, we have moved the research to Arizona, and the set-up for the animal studies is almost complete.

Task 4, effects of flow, is scheduled for year 04.

CONCLUSIONS

- ^{31}P-NMR spectroscopy of animals injected with 3-APP can be used to non-destructively, and with minimal invasiveness, determine the extracellular pH distribution of tumors *in vivo*.

- Some breast cancer cell lines exhibit a plasma membrane-associated activity of a vacuolar-type H^+-ATPase. The significance of this activity is not yet known, but there is an emerging correlation between this activity, invasiveness and multidrug resistance. A possible explanation for this correlation is that the V-ATPase activity is due to rapid endomembrane recycling.

- Rapid recycling of acidic endomembrane compartments has been theoretically proven to be capable of conferring resistance to semi-permeant drugs with alkaline pK_a values (see appended manuscript).

- The MCF-10 system holds great promise as a model for the pre-neoplastic state in our studies. Therefore, our research will continue to utilize this cell system in conjunction with the more highly transformed MCF-7 and MDA-MB-231 cells.

- ^{1}H-CSI of imidazole compounds holds promise for measurement of localized pH within tumors.

- Weak bases such as methylamine sensitize drug-resistant cells, confirming the involvement of acidic endomembrane systems in conferring drug resistance.

REFERENCES

Basolo, F. et al. (1991) *Molecular Carcinogenesis* **4**, 25-35.

Blinchikoff, H.J. and Zverev, A.I. (1986), *Filtering in the Time and Frequency Domains*, Wiley-Interscience, New York.

Brink, H.F., Buschmann, M.D., Rosen, B.R. (1989) *Comp. Med. Imag. Graph.* **13**, 93-104.

Gil, S., Zaderenzo, P., Cruz, F., Cerdan, S., Ballesteros, P. (1994) *Bioorg. Medicinal Chem.* **2**, 305-314.

Gillies, R.J., Martinez-Zaguilan, R. (1991) *J. Biol. Chem.* **266**, 1551-1556.

Gillies, R.J., Liu, Z., Bhujwalla, Z. (1994) *Am. J. Physiol.* **267**, C195-C203.

Gillies, R.J., Raghunand, N., Bhujwalla, Z.M., Glickson, J.D., Stubbs, M., Griffiths, J.R. (1995) Proc. Soc. Mag. Res., 3rd Scientific Meeting, Nice, Aug. 19-25, p1674.

Griffiths, J.R. (1991) *Br. J. Cancer* **64**, 425-427.

Lah, T.T. et al., (1992) *Intl. J. Cancer* **50**, 36-44, 1992.

LeBoeuf, R.A. (1990) *Cancer Res.* **50**, 3722-3729.

Madden, A. et al. (1991) *NMR in Biomed.* **4**, 1-11.

Martinez-Zaguilan, R. et al., (1995) *Clin. Exptl. Metastasis* (in press).

Maxwell, RJ, Khalil, AA, Horsman, MR, McCoy, C and Overgaard, J (1995) Proc. Soc. Mag. Res., 3rd Scientific Meeting, Nice, Aug. 19-25, p67.

McCoy, C.L. et al., (1995) *Br. J. Cancer* **72**, (in press).

Miller, F.R. et al. (1993) *J. Nat. Canc. Inst.* **85**, 1725-1732.

Morita, T., et al. (1992) *Mutation Res.* **268**, 297-305.

Okhuma, S., Poole, B. (1978) *Proc. Natl. Acad. Sci. USA* **75**, 3327-3331.

Rozhin, J. et al. (1994) *Cancer Res.* 54, 6517-6525.

Schlappack, O.K. et al. (1993) *Intl. J. Cancer* **64**, 663-670.

Sehested, M. et al. (1987) *J Natl. Canc. Inst.* **78**, 171-179.

Soule, H.D. et al. (1990) *Cancer Res.* **50**, 6075-6086.

Taylor, F., Smith, S.L. (1976) *Digital Signal Processing in FORTRAN*, D.C. Heath and Co.

Zaderenko, P. et al. (1994) *J. Org. Chem.* **59**, 6268-6273.

Exocytotic Transport of Weak-base Drugs from the Cytosol by Multidrug Resistant Tumor Cells: a mathematical model*

Natarajan Raghunand, Steven H. Wright,

William S. Dalton and Robert J. Gillies

Departments of Biochemistry, Internal Medicine and Physiology,

University of Arizona Health Sciences Center

1501 N Campbell Avenue

Tucson, AZ 85724

Phone: (520) 626-5050

FAX: (520) 626-2110

*Manuscript under preparation

Abstract

Resistance to chemotherapeutic agents is a major cause of treatment failure in patients with cancer. The primary mechanism leading to a multidrug resistant phenotype is overexpression of a drug efflux transporter, the p-glycoprotein (P-gp). Most work has assumed that this transporter is expressed at the plasma membrane and actively extrudes protonated organic weak bases from the cytosol. However, a number of recent reports have indicated that acidic intracellular organelles can also participate in resistance to chemotherapeutic drugs. In this communication, we have developed a general model to account for multiple mechanisms of resistance to weakly basic organic cations (e.g. anthracyclines and vinca alkaloids). This model contains terms for compartmentalized pH, dissociation constants of carrier, drug permeabilities, membrane potentials, endosomal volumes, endosomal numbers and endosomal turnover rates. The model mathematically determined that resistance to such drugs, as evidenced by lower steady-state cytosolic concentrations, can be accomplished by a number of mechanisms, including: 1) enhanced endosomal efflux involving active transport of the drug into endosomes, 2) increased endosomal turnover rates, 3) decreased endosomal pH and/or increased cytosolic pH, 4) decreased passive permeability of the protonated drug species across plasma and/or endosomal membranes and 5) decreased membrane potentials across plasma and/or endosomal membranes. All five of these mechanisms have been observed in the literature. Thus, different cells can potentially employ various combinations of these parameters to effect multi-drug resistance.

Introduction

Acquired resistance to chemotherapeutic agents is a major cause of treatment failure in patients with cancer.[1] In classical multidrug resistance (MDR), cells demonstrate simultaneous resistance to a wide range of structurally unrelated cytostatic drugs of primarily natural origin (such as anthracyclines, vinca alkaloids and epipodophyllotoxins).[2] Multidrug resistant cell lines have been obtained either from resistant tumors or from drug-sensitive cell lines which have been adapted in culture to progressively higher concentrations of the drug.[3] A majority of drug-resistant cells overexpress a variety of membrane proteins, the commonest among them being P-glycoprotein (P-gp), a 170-180 kD plasma membrane glycoprotein.[16] In addition, a "multiple-resistance protein" (MRP) has been cloned from a multidrug resistant, doxorubicin-selected cell line that did not overexpress P-glycoprotein.[5] Transfection of the cDNA encoding for P-gp[6,7] or MRP[8] have resulted in cells which display a diminished susceptibility to anthracyclines and vinca alkaloids. Drug-resistant cells have also been reported to overexpress a subunit of a vacuolar H^+-ATPase.[4,9] In order to be multidrug resistant, cells are thought to have one or both of the following features: (i) lower intracellular drug concentration,[2] possibly in conjunction with compartmentation of the drug away from the site of drug-action (the nucleus)[10], and/or (ii) altered susceptibility to the drug and increased repair mechanisms[11,12].

A lower intracellular concentration of drug may be obtained by decreased rate of uptake of drug[13,14] or an enhanced efflux of drug from the cell. In support of the enhanced efflux hypothesis, Bornmann and Roepe[15] have provided evidence that while drug efflux from drug-sensitive Chinese hamster ovary fibroblast LR73 cells could be described by one mathematical term, drug efflux from multidrug resistant MDR35 cells could only be described by two mathematical terms, one fast term similar to the one describing LR35 kinetics, and a slower term unique to the resistant cells. This suggests that a separate efflux process occurs in drug-resistant cells, which may confer resistance by lowering the intracellular concentration of the drug.

In the most widely accepted hypothesis for MDR, P-gp acts as an ATP-dependent "drug pump" to extrude drug molecules from the cell.[16] P-gp is generally considered to act on the charged form of the drug,[17] and be able to act against a concentration gradient of its substrate.[18] P-gp may be present both on the plasma membrane and in the Golgi apparatus of MDR cells.[19] P-gp alone can often not fully explain the observed MDR phenotype, prompting some researchers to postulate that MDR occurs via "complex" mechanisms.[27] Daunorubicin efflux against a cell concentration gradient has been observed in non P-gp overexpressing multidrug resistant non small-cell lung carcinoma cells, suggesting that a multidrug transporter different from P-gp is functional in these cells.[20] One such transporter is the MDR-associated protein (MRP), an ATP-binding cassette transporter overexpressed in some MDR cell lines. MRP confers MDR properties in cells transfected with MRP expression vectors.[21] However, MRP is thought to be an anion transporter, and drugs such as

anthracyclines and vinca alkaloids are cationic.

An alternate view of how MDR cells may be achieving lowered intracellular drug concentrations has drug molecules being transported into acidic vesicles, from where they are extruded from the cell by exocytosis. Sehested *et al.*[22] have reported observing greatly enhanced rates of exocytosis in multidrug resistant EAT cells, compared to their drug-sensitive parent cell line. Dubowchik *et al.*[23] have found that some imidazole compounds, in addition to raising lysosomal pH, also tended to reverse doxorubicin (DOX) resistance in HCT116-VM46, a human colon carcinoma cell line resistant to DOX. Other reports linking the alkalinization of acidic vesicles and the reversal of MDR have also been published.[24] In this context, it is interesting that some MDR cells overexpress a subunit of the vacuolar (V-type) H^+-ATPase[4]; we have observed functional expression of V-type H^+-ATPases in the plasma membranes of human tumor cells, some of which are multidrug resistant.[9] In these studies it was not determined whether the V-type H^+-ATPase was physically associated with the plasma membrane or whether the activity was an epiphenomenon of endomembrane recycling.

It is therefore likely that some MDR cell lines transport drug molecules from their cytosol into acidic vesicles and expel the drug by exocytosis. Drug uptake into these vesicles can be achieved with the activity of P-gp, or by the combined activity of V-type H^+-ATPases and an organic cation/proton antiporter. The low pH in the vesicles would cause the typical weak-base drug molecule to exist in its charged, protonated form, possible causing it to be "trapped" in the vesicle due to the low permeability of the charged molecule across the vesicular membrane.[25] In this communication, we present

a mathematical model investigating the efficacy of these proposed mechanisms of multidrug resistance.

Model Description.

Demant *et al.*[26] have published a mathematical model simulating the effects of P-gp activity, trans-membrane pH gradient and endosomal turnover on the cytosolic concentration of drug molecules, and have concluded that for exocytotic extrusion of drug molecules to be an effective mechanism of MDR, unrealistically high rates of endosomal turnover and/or unrealistically low endosomal pH values would be needed. They have therefore concluded that endosomal turnover mediated drug extrusion does not contribute to multidrug resistance. In their model, only the uncharged form of the drug molecule was taken to cross (passively or actively) any membrane. We have chosen to consider the movements of both the charged and uncharged forms of the drug molecule in our model.

Assumptions:

(i) All cells are perfect spheres of identical geometry.

(ii) Organelles other than the endosomes do not present a mass-transfer barrier to the free exchange of drug molecules between them and the cytosol. Thus, drug molecules partition between only three compartments, as shown in figure 1: the extracellular medium, the cytosol, and the endosomal vesicles.

(ii) The drug is assumed to be isotropically distributed within the cytosol.

(iii) Movement of the uncharged drug across a membrane is described by Fick's Law.

(iv) Movement of the charged drug across a membrane is described by the constant electric field equation.[27]

(v) The drug (charged and uncharged) remains in free solution, and only negligible amounts bind to membranes or macromolecules. Thus, the concentration of drug bound with DNA can be fully explained by partition with free drug.

Flux of drug (moles/time) into the cytosol:

The flux of uncharged molecules into the cytosol is described by:

$$J_{D,c} = P_{D,c} (D_e - D_c) S_{cell} \quad \textbf{(1)}$$

where $J_{D,c}$ stands for the molar flux of uncharged drug entering the cytosol from the extracellular medium, $P_{D,c}$ stands for the permeability of the uncharged drug across the plasma membrane, D_e and D_c stand for the concentration of the uncharged molecule in the extracellular medium and the cytosol respectively, and S_{cell} is the surface area of the plasma membrane.

The flux of charged molecules into the cytosol is described by:

$$J_{DH,c} = P_{DH,c} \left(\frac{V_{mc}F}{RT} \right) \left(\frac{DH_e - DH_c \exp\left(\frac{V_{mc}F}{RT} \right)}{\exp\left(\frac{V_{mc}F}{RT} \right) - 1} \right) S_{cell} \quad \textbf{(2)}$$

where $J_{DH,c}$ stands for the molar flux of protonated drug entering the cytosol through the plasma membrane, $P_{DH,c}$ stands for the permeability of the charged drug molecule

across the plasma membrane, V_{mc} is the plasma membrane potential (always negative inside), F is Faraday's constant, T is the absolute temperature (Kelvin), and DH_e and DH_c are the concentrations of the protonated drug in the extracellular medium and the cytosol, respectively.

Active transport of protonated drug into the endosome:

Protonated drug may be transported across the endosomal membrane either along its electrochemical gradient, or by active transport. This active transport could be ATP-dependent, as is the case with P-gp mediated active transport.[28] Active transport of organic cations into endosomes may also be driven by the proton-gradient across the endosomal membrane.[46,47] This represents an energy-dependent mechanism for drug transport into the endosomes, since the H^+ gradient across the endosomal membrane is maintained by energy-dependent H^+-ATPases.[29] Spoelstra *et al.*[30] have described the kinetics of P-gp by means of Michaelis-Menten type kinetics, with the rate of efflux being dependent only on the cytosolic concentration of the charged drug molecule. P-gp mediated drug efflux has been reported to be insensitive to pH, but an organic cation/H^+ antiporter acting on the endosomal membrane could be pH-sensitive.[31,46,47] The following equation, a simplification of a more general rate equation for antiporters given by Stein and Leib[32], was used to describe the dependence of transporter kinetics on DH_c and pH_v. Note that this form of rate equation permits us to model the active transporter as either P-gp or as a general organic cation/H^+ antiporter, simply by altering the values we choose for k_{DH} and k_H.

$$v_{DH,v} = \frac{V_T[DH^+]_c[H^+]_v}{(k_{DH} + [DH^+]_c)(k_H + [H^+]_v)} \quad (3)$$

where,

$V_T = N_T \cdot k_T$,

N_T = the number of transporter molecules per unit endosomal membrane surface area,

k_T = the maximum transport rate for one transporter molecule

(moles DH^+ transported/time/transporter molecule),

k_{DH} = the dissociation constant of the DH^+/transporter complex, and,

k_H = the dissociation constant of the H^+/transporter complex,

$[H^+]_v$ = the free H^+ concentration in the endosomes.

Flux of drug (moles/time) into the endosome from the cytosol:

Passive movement of uncharged molecules into endosomes can be described by:

$$J_{D,v} = P_{D,v} (D_c - D_v) S_{endo} N_{endo} \quad (4)$$

where $J_{D,v}$ is the combined molar flux of uncharged drug into all the endosomes from the cytosol; $P_{D,v}$ is the permeability of the uncharged drug molecule across the endosomal membrane; D_v is the concentration of the uncharged molecule in the endosomes; S_{endo} is the surface area of a single endosome; and N_{endo} is the total number of endosomes per cell.

The movement of charged molecules into the endosomes is described by:

$$J_{DH,v} = P_{DH,v}\left(\frac{V_{mv}F}{RT}\right)\left(\frac{DH_v - DH_c\exp\left(\frac{-V_{mv}F}{RT}\right)}{\exp\left(\frac{-V_{mv}F}{RT}\right) - 1}\right) S_{endo}\, N_{endo}$$

$$+ \frac{V_T[DH^+]_c[H^+]_v}{(k_{DH} + [DH^+]_c)(k_H + [H^+]_v)} S_{endo}\, N_{endo} \qquad \textbf{(5)}$$

where $J_{DH,v}$ is the molar flux of protonated drug entering the endosome through the endosomal membrane; $P_{DH,v}$ stands for the permeability of the charged drug molecule across the endosomal membrane; V_{mv} is the endosomal membrane potential (always positive inside); and DH_v is the concentration of the protonated drug in the endosomes.

Steady-state requirements:

All parameters are modeled to determine steady-state values. Thus, the concentrations of drug in the cytosol and endosomes do not change with time. Therefore, flux from extracellular medium into the cytosol = flux into endosomes from cytosol:

$$J_{D,c} + J_{DH,c} = J_{D,v} + J_{DH,v} \qquad \textbf{(6)}$$

and the flux from cytosol into endosomes = flux of drug out of cell by exocytosis:

$$J_{D,v} + J_{DH,v} = (D_v + DH_v)T_{vc}V_{endo}N_{endo} \qquad \textbf{(7)}$$

where V_{endo} is the volume of a single endosome, and T_{vc} is the fractional endosomal volume exocytosed per unit time (the "turnover rate").

Equilibrium requirements:

Since the unprotonated and protonated drug molecules exist in equilibrium in all three compartments, we have the following equations:

$$\textit{Extracellular Medium}: \quad D_e = DH_e \cdot 10^{(pH_e - pK_a)} \tag{8}$$

$$\textit{Cytosol}: \quad D_c = DH_c \cdot 10^{(pH_c - pK_a)} \tag{9}$$

$$\textit{Endosome}: \quad D_v = DH_v \cdot 10^{(pH_v - pK_a)} \tag{10}$$

Overall conservation of drug:

There must be a conservation of drug-mass over the extracellular medium, the cytosol, and the endosomes. Thus, we have the equation:

$$(D_e + DH_e)V_{ext} + (D_c + DH_c)V_{cyto} + (D_v + DH_v)V_{endo}N_{endo} = [Drug]_{initial}V_{ext}$$

where V_{ext} is the extracellular (medium) volume, and $[Drug]_{initial}$ is the initial extracellular drug concentration. Since only a small fraction of the drug is contained in the cytosol and the endosomes, this equation may be approximated to:

$$D_e + DH_e = [Drug]_{initial} \tag{11}$$

Equations 1-2 and 4-11 are linear equations and may be solved simultaneously for the 10 unknowns $J_{D,c}$, $J_{DH,c}$, $J_{D,v}$, $J_{DH,v}$, $[D_e]$, $[DH_e]$, $[D_c]$, $[DH_c]$, $[D_v]$ and $[DH_v]$.

Model Parameters.

The following parameter value ranges were chosen from literature values and tested in this model:

(i) $[Drug]_{initial}$, initial extracellular drug concentration, 1μM to10μM;[33,34]

(ii) pH_e, extracellular pH, 6.5 to 7.5;[35]

(iii) pH_c, cytosolic pH, 6.5 to 7.5;[36]

(iv) pH_v, average endosomal pH, 4.5 to 6.5;[37]

(v) pK_a, acid dissociation constant of the drug, 7.0 to 9.0;[40,54]

(vi) $P_{D,c}$ ($P_{D,v}$), permeability of uncharged drug specie, $1x10^{-9}$ to $1x10^{-7}$ m/sec;[38,39,54]

(vii) $P_{DH,c}$ ($P_{DH,v}$), permeability of charged drug specie, 0.01% to 0.5% of $P_{D,c}$ ($P_{D,v}$); (Boron and Roos ?)

(viii) V_{mc}, plasma membrane potential, -30 mv to -80 mv;[41,42]

(ix) V_{mv}, endosomal membrane potential, +30 mv to +80 mv;[43?]

(x) N_{endo}, number of endosomes, 50 to 200;[44]

(xi) d_{cell}, diameter of the cell, assumed to be 15 μm;

(xii) $V_{endo} \cdot N_{endo}$, total endosomal volume, 0.5% to 2% of cell volume;[44]

(xiii) k_{DH}: dissociation constant of protonated drug from carrier. Wright and Wunz[46] have studied organic cation/H^+ antiport in brush-border and basolateral membrane vesicles taken from the rabbit renal cortex, and have reported K_m values in the region of 0.15mM to 0.37mM for the uptake of tetraethylammonium into the vesicles. Guiral *et al.*[45] have investigated the kinetics of P-glycoprotein, and report an apparent K_m value of 1.5μM for the transport of daunorubicin. We have therefore varied the value of this constant

between 1μM and 0.5 mM.

(xiv) k_H: dissociation constant of protons from carrier, 10^{-8} to 10^{-7} M. Based on the work of Wright and Wunz[46], we have made the putative endosomal drug pump relatively insensitive to the endosomal pH.

(xv) V_T: the values of V_T were chosen so as to give rates of active transport of drug into the endosomes that were an order of magnitude higher than rates of passive diffusion of the uncharged drug molecule into the endosomes.

(xvi) T_{vc}, the fraction of endosomal volume exocytosed per second, 0 sec^{-1} to 10^{-4} sec^{-1} (0.0% $hour^{-1}$ to 36 % $hour^{-1}$).[22]

The general equation, combining equations 1-2 and 4-11 were solved using Mathcad 5.0 (Mathsoft Inc.) with the above values of the parameters.

Results.

We have assumed that all endosomes are identical, and spend identical lengths of time in the cytosol before exocytosing. In reality, there may be a distribution of "residence times" of the endosomes in the cytosol. In addition, pH_v may be a function of the residence time, with the consequence that newly formed endosomes may have an internal pH not too different from the extracellular pH, and older endosomes may become increasingly acidic with "age". This would mean that the ability of an endosome to sequester drug molecules will depend on its age. At steady-state, one would have a fixed "residence time distribution" (RTD)[48] of the endosomes in the cytosol: individual endosomes would undergo changes in pH, but the population as a whole would retain a

constant average pH_v, and average values of D_v and DH_v. Given the RTD, it is possible to calculate the appropriately weighted means of the distributions of pH_v, D_v and DH_v.[48] Since we might not always have the means to obtain the residence time distribution of endosomes in a cell, we have assumed average and uniform distributions of pH_v, D_v and DH_v in the above model. This assumption does not qualitatively alter the behavior of the model. Equations 1, 2, and 4-11 may now be solved simultaneously for the unknowns $J_{D,c}$, $J_{DH,c}$, $J_{D,v}$, $J_{DH,v}$, $[D_e]$, $[DH_e]$, $[D_c]$, $[DH_c]$, $[D_v]$ and $[DH_v]$. In addition, we have assumed that the drug is distributed homogeneously in the intracellular volume. This is probably not the case, and there are published reports of lowered nuclear levels of drug in MDR cells.[10,49,50] However, the concentration of drug in the nucleus can be described by a partition equilibrium with the cytosol. Thus, lowered cytosolic levels will lead to lower nuclear levels.

For a given drug and given growth conditions, there are at least 7 cellular parameters which can affect the ability of the cell to transport drug molecules out of its cytosol: (1) the endosomal turnover rate T_{vc}; (2) the average endosomal pH, pH_v; (3) the total volume contained in the endosomes, $V_{endo} \cdot N_{endo}$,; (4) the number of endosomes per cell, N_{endo}; (5) the activity (V_T) of the organic cation/H^+ antiporter on endosomal membranes: the cell may alter this activity by altering the number of antiporter molecules expressed; (6) k_{DH}, the dissociation constant of the antiporter-protonated drug molecule complex, and (7) k_H, the dissociation constant of the antiporter-proton complex. We have utilized the present mathematical model to investigate the effectiveness of changes in these parameters in altering the drug concentration in the

cytosol relative to the drug concentration present outside the cell. Figures 2-4 show the effect of varying these parameters on the ratio of cytosolic to extracellular drug concentration (i.e. the "drug ratio"). In all figures, the drug ratio is shown as a function of endosomal pH and endosomal turnover rate.

Case I. Vesicular turnover, with active transport of drug into endosomes. The first case examines a system wherein endosomal turnover and active transport of drugs into endosomes collaborate to reduce cytosolic drug concentrations. The drug and cell line had the characteristics listed in table I. → page 24 The results of these analyses are given in Figures 2(a) - 2 (d). These four figures investigate the effect of endosomal volumes on the drug ratio by varying the number and total volume of endosomes in the cell. In Figures 2(a) and 2(b) there are 200 endosomes per cell, and in Figures 2(c) and 2(d) there are 100 endosomes per cell. In Figures 2(a) and 2(c) endosomal volume is 1.0% of the cell volume, whereas in Figures 2(b) and 2(d) endosomal volume is 0.5% of the cell volume.

As illustrated in these figures, the total volume of the endosomes, the turnover rate, and the average endosomal pH all have profound effects on the drug ratio. Cytosolic drug concentrations are relatively unaffected by the number of endosomes, provided the volume is held constant. As shown in figure 2(a), at moderate rates of endosomal turnover (18% per hour) and endosomal pH (5.6), the cytosolic drug concentration can be reduced to 40% that found in the extracellular medium. With rapid turnover rates (36% per hour) and low pH values (4.4), the ratio can be reduced to 8%. Note also that, by extrapolation, increasing endosomal turnover rates further will

not significantly reduce cytosolic drug concentrations. Reducing the total endosomal volume (cf. figures a and b, or c and d), reduces the effectiveness of this mechanism by up to a factor of two. Note that this effect is maximal only at the highest turnover rates. There is very little effect if the total volume of endosomes is kept constant, yet the total number of endosomes is changed (cf. figures a and c, or b and d).

Case II. No endosomal turnover, with active transport of drug into endosomes. Since most common chemotherapeutic drugs are weak bases, a cytosolic pH that is more alkaline than the extracellular pH will result in a limited exclusion of the drug from the cytosol. In addition, some of the drug will be sequestered in acidic vesicles. An extrapolation of the turnover rate in figures 2(a)-2(d) to zero reveals that in the absence of endosomal turnover, the cytosolic drug concentration will still be up to 70% of the extracellular drug concentration, for chronic exposure of the cell to the drug. Thus, turnover of acidic vesicles is required for drug resistance.

Case III. Vesicular turnover, with no active drug transport. Figure 3 shows model calculations using the same values of all parameters as in figure 2(a), except for V_T, which is set to zero to simulate the absence of active drug efflux from the cytosol into the endosomes. Once again, it is clear that the cytosolic drug concentration is not lowered significantly, even by substantial rates of endosomal turnover. Thus, active transport of drug into endosomes is essential for drug resistance.

Case IV. Vesicular turnover with active transport of drug at plasma membrane, but not at endosomal membrane.

In order to simulate the activity of P-gp at the plasma membrane, equation 2 was

modified by dividing the DH_e term by 100, thus conferring a 100-fold lower permeability for charged drug molecules entering the cytosol, without altering the permeability of the plasma membrane for drug molecules leaving the cytosol. In addition, V_T was set to zero to simulate the absence of active transport of drug into endosomes. The results of these analyses are shown in figure 4. As expected, cytosolic drug concentrations are independent of endosomal turnover rate and pH. Surprisingly, there is almost no reduction in cytosolic drug concentrations as compared to case III (figure 3).

Discussion.

Requirements for MDR. It is thus clear that some form of active transport combined with turnover of the endosomal vesicles is required for the cytosolic drug concentration to be substantially lower than the extracellular drug concentration at steady-state. Simple alterations in cytosolic pH or number and volume of endosomes, in the absence of turnover and active transport, do not significantly lower the cytosolic drug concentration.

Effect of pH. A more acidic pH_e results in a lower ratio of cytosolic to extracellular drug concentration (henceforth, the "drug ratio"), all else remaining the same. This merely reflects the partitioning of the weak-base drug molecule into the more acidic compartment. This is in agreement with previous reports of a more alkaline cytosolic pH being associated with a greater degree of drug resistance.[51] Also apparent from figures 2-4 is that a lower average endosomal pH results in a lower drug ratio.

Design of Drug Molecules. Figure 5 shows the results of a simulation using conditions

identical to those used in figure 2(a), but for a drug of pK_a 9.0: a comparison of figures 2(a) and 5 reveals that the cell is dramatically more resistant to drugs with more alkaline acid-dissociation constants. We also see that vesicular turnover is required for the cell to achieve any degree of drug-resistance, regardless of the drug pK_a.

Figure 6 shows a simulation with conditions identical to those used in figure 3, but for a drug of pK_a 9.0: clearly, active transport of the drug into the endosomes is required for drug-resistance, even for drug molecules with higher pK_a values.

Figure 7 displays the results of a simulation with conditions identical to those used in figure 4, but for a drug with pK_a 9.0: we can conclude from figures 4 and 7 that a drug-pump located at the plasma membrane will have only a limited ability to reduce the cytosolic concentration of weak-base drug molecules, and will be substantially more effective when localized at the endosomal membrane.

Drug permeabilities. Under the conditions tested, at steady-state, there is a net flow inward at the plasma membrane of both protonated and unprotonated drug molecules. At the endosomal membrane, there is a net flow into the endosome from the cytosol of unprotonated drug molecules, while the net flow of protonated drug molecules is into the cytosol from the endosomes. With that in mind, let us consider the results of the simulation as the various permeability coefficients are varied. Lowering influx of the protonated specie is effectively equivalent to increased efflux of the protonated specie. A lower $P_{DH,c}$ does not significantly lower the drug ratio: therefore, active export of the drug at the plasma membrane will not be significantly useful in conferring drug resistance to the cell. A lower $P_{DH,v}$, however, sharply lowers the drug ratio, indicating

the usefulness of active transport of drug into endosomes from the cytosol. A lower $P_{D,c}$ results in a sharply lowered drug ratio, indicating that modification of plasma membrane permeabilities could also be a potential mechanism of drug resistance, as suggested by some.[13,14,52] The drug ratio is insensitive to a 10-fold increase in $P_{D,v}$ for a drug of pK_a 9.0 and moderately sensitive in the case of a drug with pK_a 8.0, possibly because most weak-base drug molecules in acidic vesicles would be in their protonated form.

Membrane potentials. A lower plasma membrane potential results in a lowered drug ratio. This is in agreement with the correlation made by some groups between a less negative plasma membrane potential and increased drug resistance.[41,42,53] Verapamil and cyclosporin A, agents reversing MDR, have been shown to reduce the plasma membrane potential of the resistant cells.[41] A less positive endosomal membrane potential also results in a lowering of the drug ratio, by reducing the efflux of protonated drug molecules into the cytosol from the endosomes down their electrochemical gradient.

Conclusions. The general model developed here illustrates that there are multiple mechanisms capable of lowering cytosolic concentrations of weak base drugs. these include: 1) enhanced endosomal efflux involving active transport of the drug into the endosomes, 2) increased endosomal turnover rates, 3) decreased endosomal pH and/or increased cytosolic pH, 4) decreased passive permeability of the protonated drug species across the endosomal membrane, and, 5) decreased membrane potentials across plasma and/or endosomal membranes. All of these mechanisms have been observed in the literature. Thus, different cells can potentially employ

various combinations of these parameters to effect multi-drug resistance.

References

1. Dalton, W. S. (1994) *Curr. Opinion Oncol.* **6:** 595-600.

2. Nielsen, D and Skovsgaard, T. (1992) *Biochim. Biophys. Acta* **1139:** 169-183.

3. Clynes, M. (1993) *In Vitro Cell. Dev. Biol.* **29A:** 171-179.

4. Ma, L. and Center, M. S. (1992) *Biochem. Biophys. Res. Commun.* **182:** 675-681.

5. Cole, S. P. C., Bhardwaj, G., Gerlach, J. H., Mackie, J. E., Grant, C. E., Almquist, K. C., Stewart, A. J., Kurz, E. U., Duncan, A. M. V, and Deeley, R. G. (1992) *Science* **258:** 1650-1658.

6. Pastan, I., Gottesman, M. M., Ueda, K, Lovelace, E., Rutherford, A. V., and Willingham, M. C. (1988) *Proc. Natl. Acad. Sci. USA* **85:** 4486-4498.

7. Ueda, K., Cardarelli, C., Gottesman, M. M., and Pastan, I. (1987) *Proc. Natl. Acad. Sci. USA* 84: 3004-3011.

8. Grant, C. E., Valdimarsson, G., Hipfner, D. R. Almquist, K. C., Cole, S. P. C., and Deeley, R. G. (1994) J. Immunol. Methods **65:** 55-61.

9. Martinez-Zaguilan, R., Martinez, G. M., Rojas, B., Dalton, W. S., and Gillies, R. J. (1995) (in prep.).

10. Schuurhuis, G. J., Broxterman, H. J., de Lange, J. H. M., Pinedo, H. M., van Heijningen, T. M. H., Kuiper, C. M., Scheffer, G. L., Scheper, R. J., van Kalken, C. K., Baak, J. P. A and Lankelma, J. (1991) *Br. J. Cancer* **64:** 857-861.

11. De Isabella, P., Capranico, G., and Zunino, F. (1991) *Life Sciences* **48:** 2195-2205.

12. Klohs, W. D., Steinkampf, R. W., Leopold, W. R., and Fry, D. W. (1987) *Proc. Am. Assoc. Cancer Res.* **28:** 298.

13. Klohs, W. D., Steinkampf, R. W., Havlick, M. J., and Jackson, R. J. (1986) *Cancer Res.* **46:** 4352-5356.

14. Klohs, W. D., Steinkampf, R. W., Besserer, J. A., and Fry, D. W. (1987) *Cancer Lett.* **31:** 253-260.

15. Bornemann, W. G. and Roepe, P. D. (1994) *Biochemistry* **33:** 12665-12675.

16. Gottesman, M. M. and Pastan, I. (1993) *Annu. Rev. Biochem.* **62:** 385-427.

17. Spoelstra, E. C., Dekker, H, Schuurhuis, G. J., Broxterman, H. J., and Lankelma, J (1991) *Biochem. Pharmacol.* **41:** 349-359.

18. Ruetz, S. and Gros, P. (1994) Trends Pharmacol. Sci. 15: 260-263.

19. Molinari, A., Cianfriglia, M., Meschini, S., Calcabrini, A., and Arancia, G. (1994) *Int. J. Cancer* **59:** 789-795.

20. Mulder, H. S., Lankelma, J., Dekker, H., Broxterman, H. J., and Pinedo, H. M. (1994) *Int. J. Cancer* **59:** 275-281.

21. Leier, I., Jedlitschky, G., Buchholz, U., Cole, S. P. C., Deeley, R. G., and Keppler, D. (1994) *J. Biol. Chem.* **269:** 27807-27810.

22. Sehested, M., Skovsgaard, T., van Deurs, B., and Winther-Neilsen, H. (1987) *J. Natl. Cancer Inst.* **78:** 171-179.

23. Dubowchik, G. M., Padilla, L., Edinger, K., and Firestone, R. A. (1994) *Biochim. Biophys. Acta* **1191:** 103-108.

24. Sehested, M., Skovsgaard, T., and Roed, H. (1988) *Biochem. Pharmacol.* **37:** 3305-

3310.

25. Simon, S. M. and Schindler, M. (1994) *Proc. Natl. Acad. Sci. USA* **91:** 3497-3504.

26. Demant, E. J. F., Sehested, M., and Jensen, P. B. (1990) B*iochim. Biophys. Acta* **1055:** 117-125.

27. Goldman, D. E. (1943) *J. Gen. Physiol.* **27:** 37-60.

28. Schlemmer, S. R. and Sirotnak, F. M (1994) *J. Biol. Chem.* **269:** 31059-31066.

29. Forgac, M. (1992) *J. Exp. Biol.* **172:** 155-169.

30. Spoelstra, E. C., Westerhoff, H. V., Dekker, H., and Lankelma, J (1992) *Eur. J. Biochem.* **207:** 567-579.

31. Pritchard, J. B., Sykes, D. B., Walden, R., and Miller, D. S. (1994) *Am. J. Physiol.* **266:** F966-976.

32. Stein, W. D. and Leib, W. R. (1986) "Transport and Diffusion across Cell Membranes", Acad. Press..

33. Taylor, C. W., Dalton, W. S., Parrish, P. R., Gleason, M. C., Bellamy, W. T., Thompson, F. H., Roe, D. J., and Trent, J. M. (1991) *Br. J. Cancer* **63:** 923-929.

34. Awasthi, S., Sharma, R., Awasthi, Y. C., Belli, J. A., and Frenkel, E. P. (1992) *Cancer Lett.* **63:** 109-116.

35. Gillies, R. J., Liu, Z., and Bhujwalla, Z. (1994) *Am. J. Physiol.* **267:** C195-C203.

36. Zaguilan-Martinez, R., Lynch, R. M., Martinez, G. M., and Gillies, R. J. (1993) *Am. J. Physiol.* **265:** C1015-C1029.

37. Roederer, M., Bowser, R., and Murphy, R. F. (1987) *J. Cell. Physiol.* **131:** 200-209.

38. Dalmark, M. and Hoffman, E. K. (1983) *Scand. J. Clin. Lab. Invest.* **43:** 241-248.

39. Dordal, M. S., Winter, J. N., and Atkinson, A. J. Jr. (1992) *J. Pharm. and Exp. Therapeutics* **263:** 762-766.

40. Skovsgaard, T. and Nissen, N. I. (1982) *Pharm. and Therapeutics* **18:** 293-311.

41. Vayuvegula, B., Slater, L., Meador, J. and Gupta, S. (1988) *Cancer Chemother. Pharmacol.* **22:** 163-168.

42. Hasmann, M., Valet, G. K., Tapiero, H., Treverrow, K., and Lampidis, T. (1989) *Biochem. Pharmacol.* **38:** 305-312.

43. Praet, M., Defrise-Quertain, F., and Ruysschaert, J. M. (1993) *Biochim. Biophys. Acta* **1148:** 342-350.

44. Sehested, M. , Skovsgaard, T., van Deurs, B., and Winther-Neilson, H. (1987) *Br. J. Cancer*, **56:** 747-751.

45. Guiral, M., Viratelle, O., Westerhoff, H. V., and Lankelma, J. (1994) *FEBS Lett.* **346:** 141-145.

46. Wright, S. H. and Wunz, T. M. (1987) *Am. J. Physiol.* **253:** F1040-F1050.

47. Van Dyke, R. W., Faber, E. D., and Meijer, D. K. F. (1992) *J. Pharm. Exp. Therap.* **261:** 1-11.

48. Levenspiel, O. (1972) "Chemical Reactor Engineering", Wiley, N.Y.

49. Toffoli, G., Simone, F., Gigante, M., and Boiocchi, M. (1994) *Biochem. Pharmacol.* **48:** 1871-1881.

50. Slapak, C. A., Mizunuma, N., and Kufe, D. W. (1994) *Blood* **84:** 3113-3121.

51. Keizer, H. G. and Joenje, H. (1989) *J. Natl. Cancer Inst.* **81:** 706-709.

52. Beck, W. T. (1987) *Biochem. Pharmacol.* **36:** 2879-2887.

53. Roepe, P. D., Wei, L. Y., Cruz, J., and Carlson, D. (1993) *Biochemistry* **32:** 11042-11056.

54. Dalmark, M. (1981) *Scand. J. Clin. Lab. Invest.* **41:** 633-639.

Table I. Parameter Characteristics for case No. 1

Permeability of unprotonated drug molecules, $P_{D,c} = P_{D,v} = 1x10^{-8}$ m/sec

Permeability of protonated drug molecules $P_{DH,c} = P_{DH,v}$ = 1x10-11 m/sec

Drug pK_a = 8.0, V_{mv} = +50 mv

Extracellular drug concentration = 1μM, k_{DH} = 150μM.

Extracellular pH = 7.0, $k_H = 10^{-7.5}$ M

Cytosolic pH = 7.2 $V_T = 1.5x10^{-8}$ moles/(m^2-sec)

V_{mc} = -50 mv

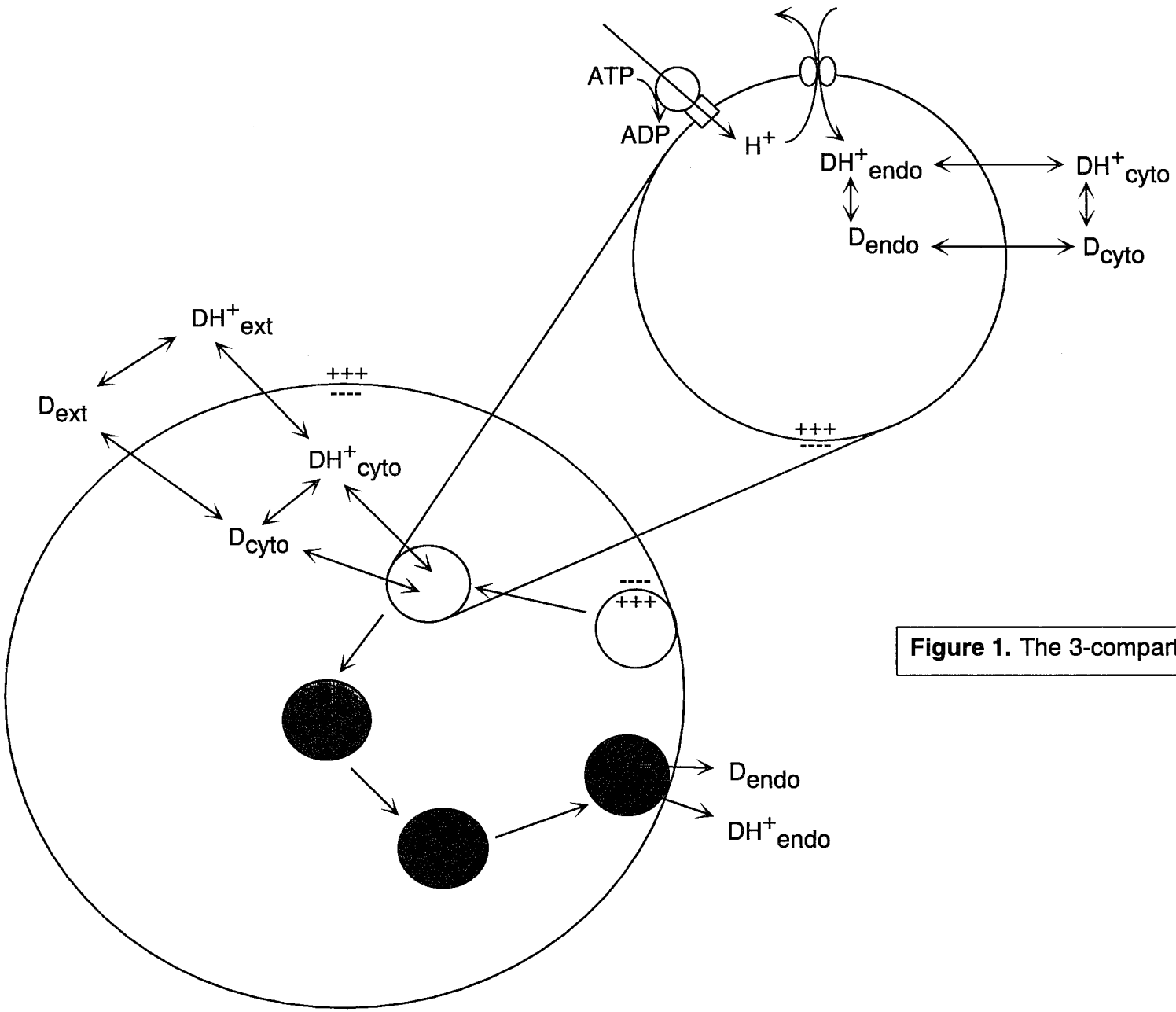

Figure 1. The 3-compartment model.

Figure 2(a)

Drug pK_a = 8.0; $P_{DH,v}$ = 1x10^{-11} m/sec; $P_{DH,c}$ = 1x10^{-11} m/sec
k_H = 10$^{-7.5}$ M; V_T = 1.5x10^{-8} moles/(m^2-sec); k_{DH} = 150μM
Number of Endosomes = 200
Total Endosomal Volume = 1.0% of Cell Volume

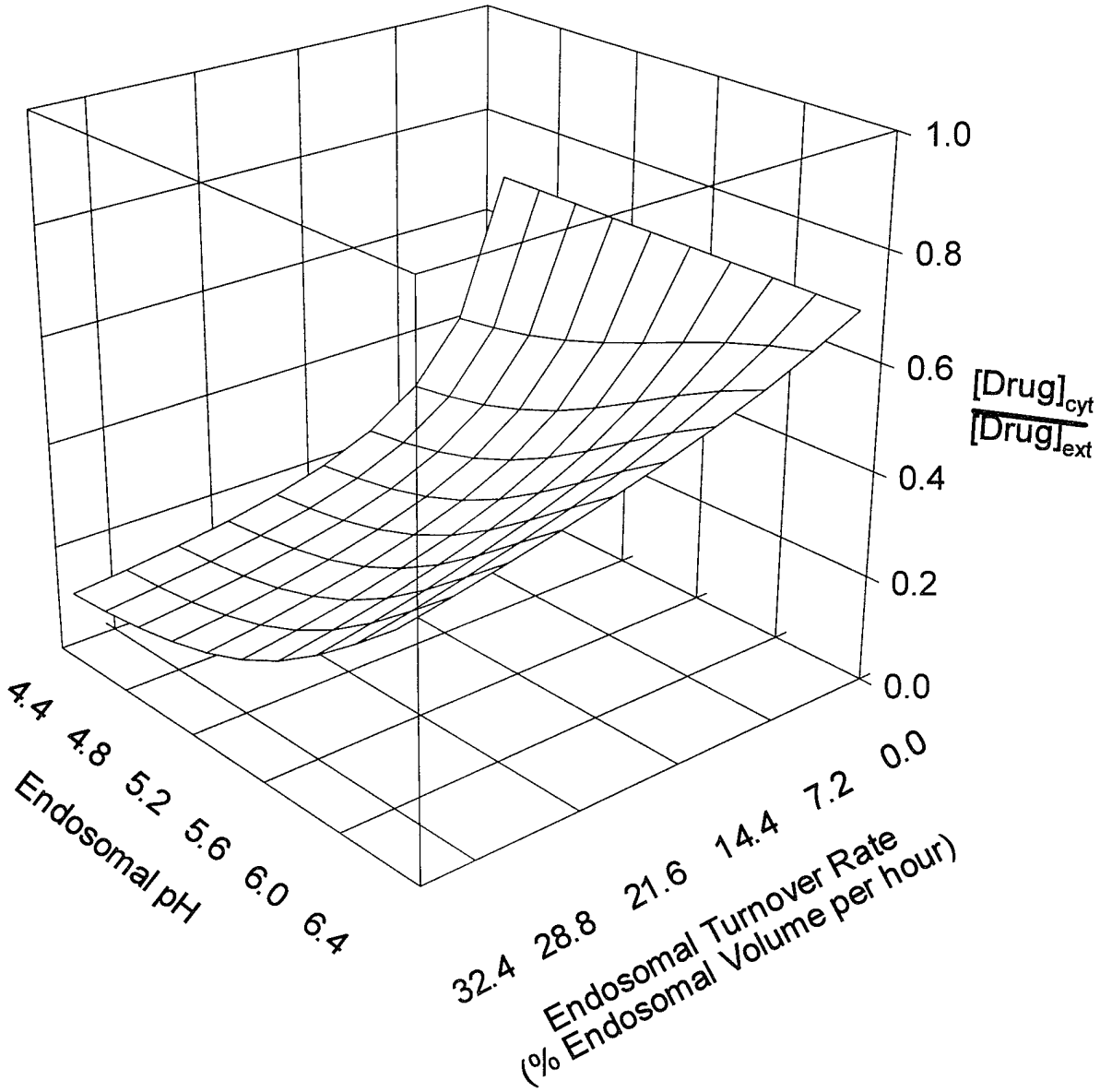

Figure 2(b)

Drug pK_a = 8.0; $P_{DH,v}$ = 1x10^{-11} m/sec; $P_{DH,c}$ = 1x10^{-11} m/sec
k_H = 10$^{-7.5}$ M; V_T = 1.5x10^{-8} moles/(m^2-sec); k_{DH} = 150μM
Number of Endosomes = 200
Total Endosomal Volume = 0.5% of Cell Volume

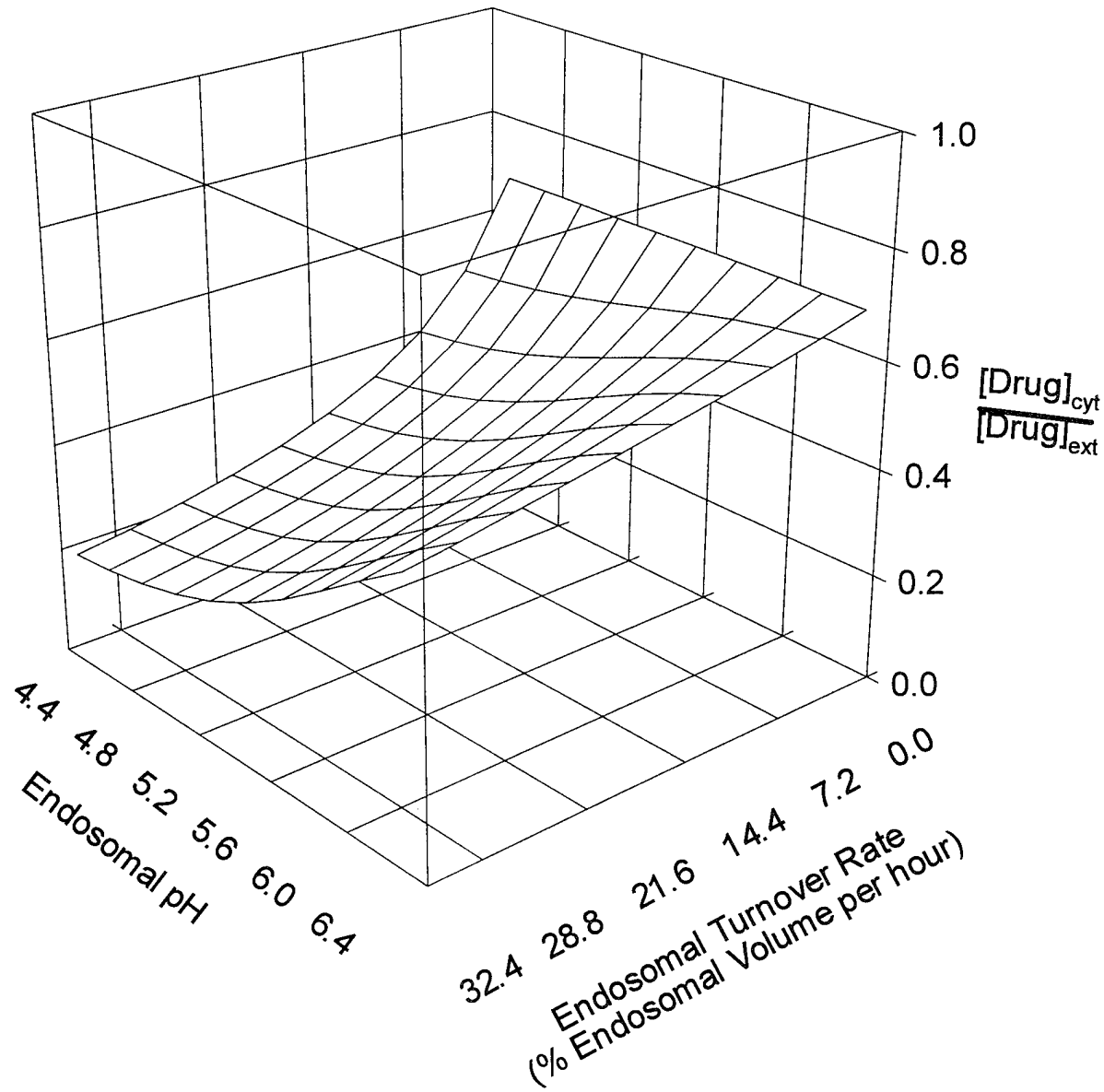

Figure 2(c)

Drug pK_a = 8.0; $P_{DH,v}$ = 1x10^{-11} m/sec; $P_{DH,c}$ = 1x10^{-11} m/sec
k_H = 10$^{-7.5}$ M; V_T = 1.5x10^{-8} moles/(m^2-sec); k_{DH} = 150μM
Number of Endosomes = 100
Total Endosomal Volume = 1.0% of Cell Volume

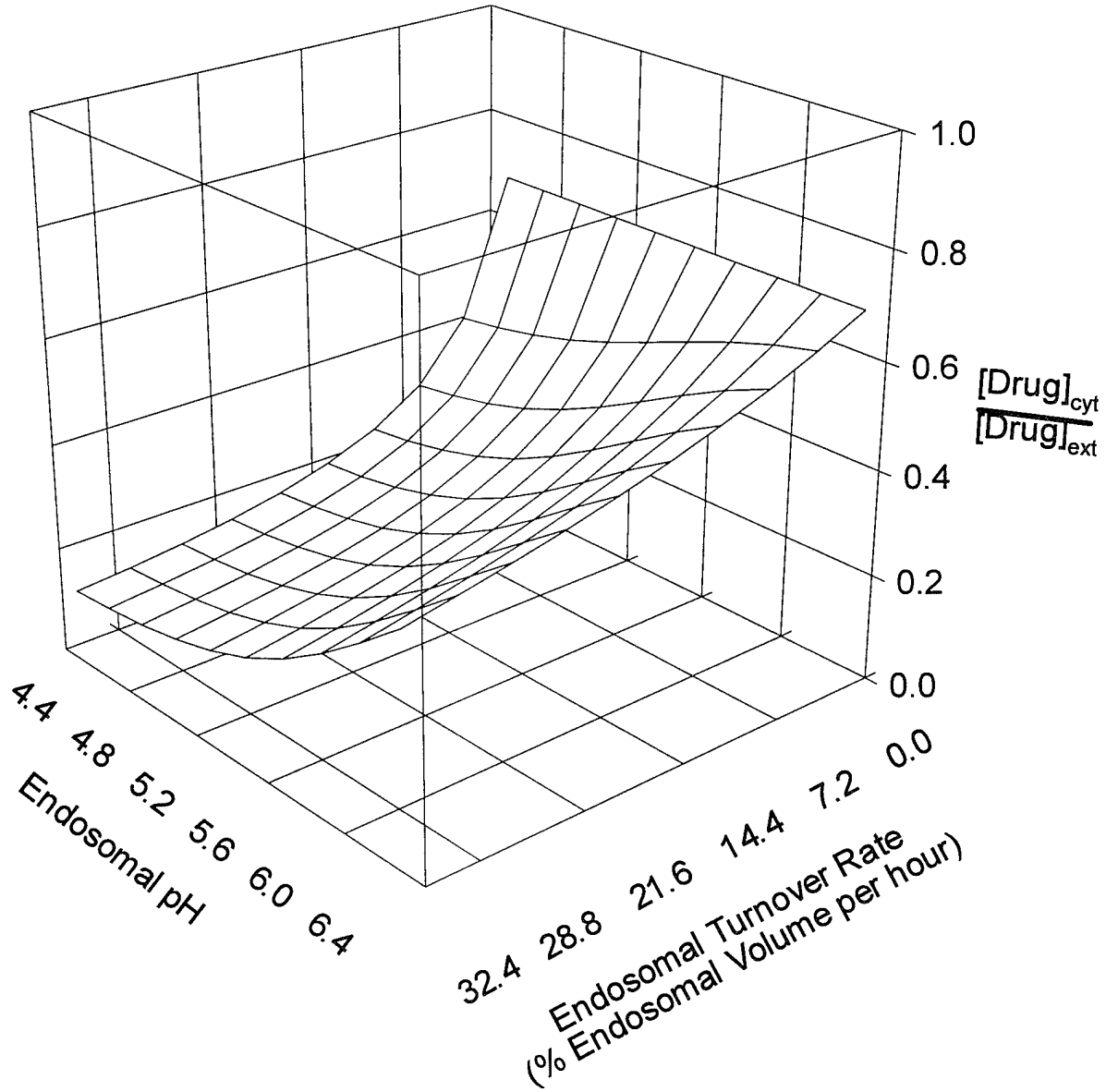

Figure 2(d)

Drug pK_a = 8.0; $P_{DH,v}$ = 1x10^{-11} m/sec; $P_{DH,c}$ = 1x10^{-11} m/sec
k_H = 10$^{-7.5}$ M; V_T = 1.5x10^{-8} moles/(m^2-sec); k_{DH} = 150μM
Number of Endosomes = 100
Total Endosomal Volume = 0.5% of Cell Volume

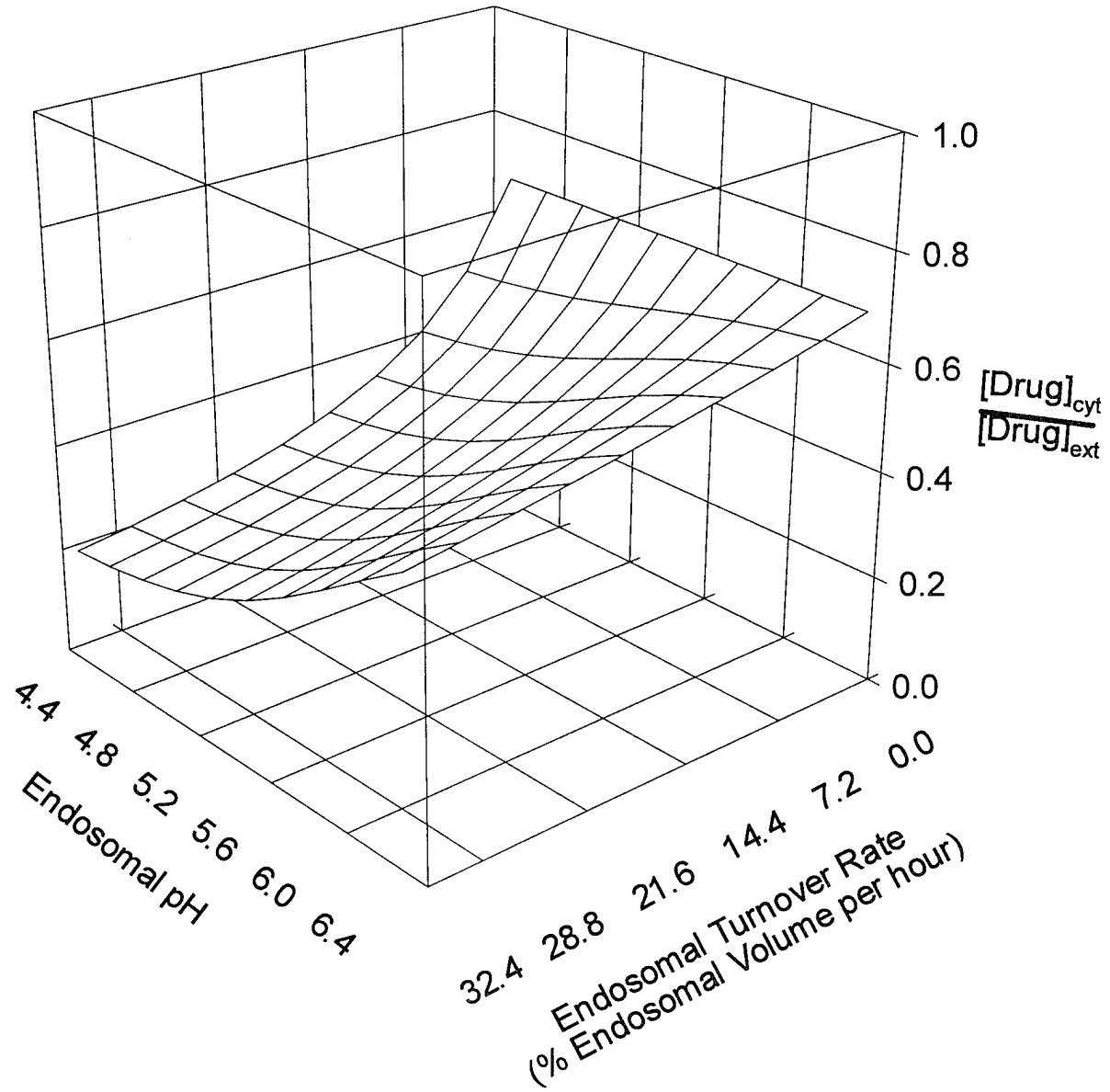

Figure 3

Drug pK_a = 8.0; $P_{DH,v}$ = 1x10^{-11} m/sec; $P_{DH,c}$ = 1x10^{-11} m/sec
k_H = 10$^{-7.5}$ M; V_T = 0.0x10^{-8} moles/(m^2-sec); k_{DH} = 150μM
Number of Endosomes = 200
Total Endosomal Volume = 1.0% of Cell Volume

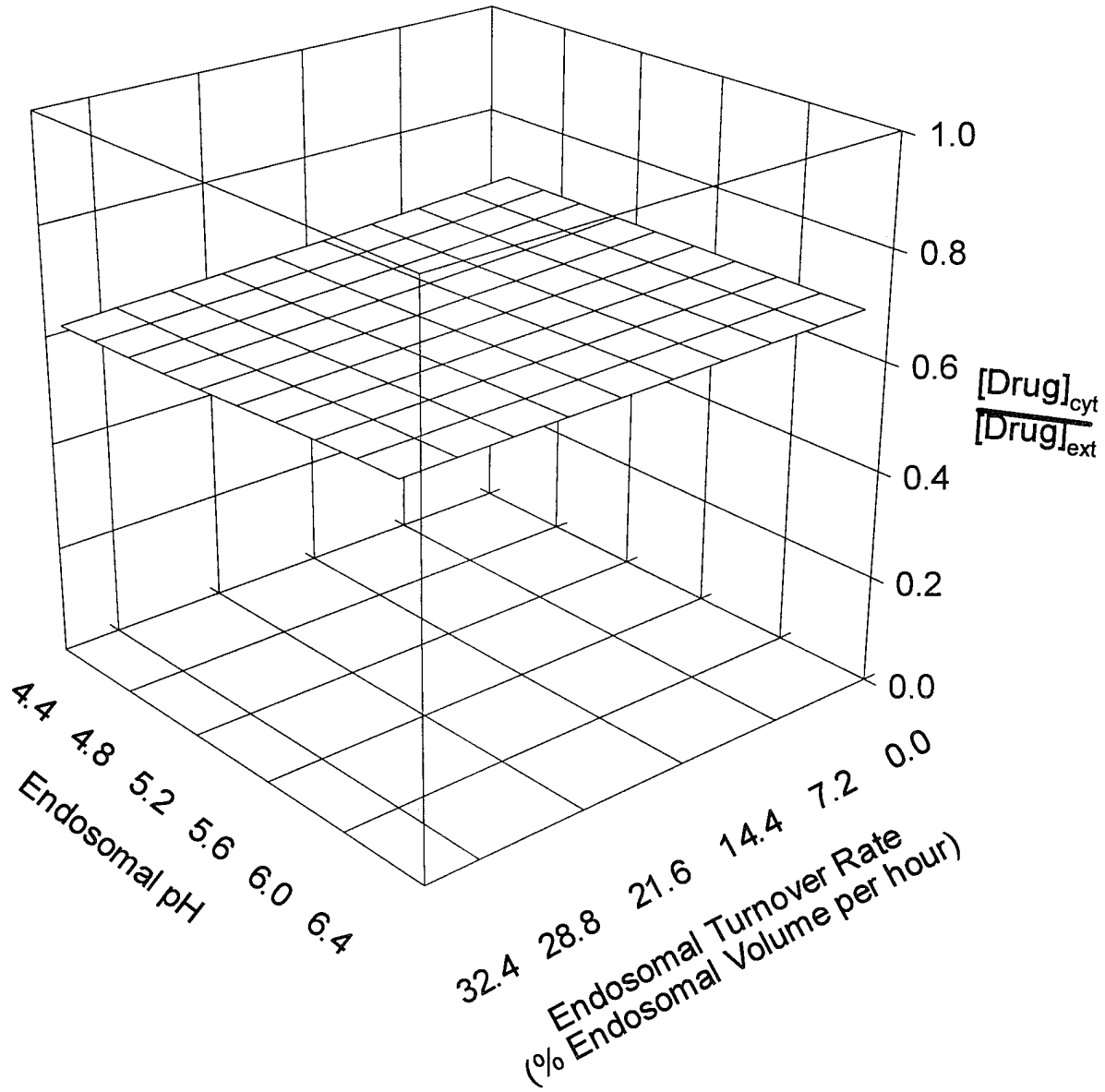

Figure 4

Drug pK_a = 8.0; $P_{DH,v}$ = 1x10^{-11} m/sec; $P_{DH,c}$ = 1x10^{-13} m/sec
k_H = 10$^{-7.5}$ M; V_T = 0.0x10^{-8} moles/(m^2-sec); k_{DH} = 150μM
Number of Endosomes = 200
Total Endosomal Volume = 1.0% of Cell Volume

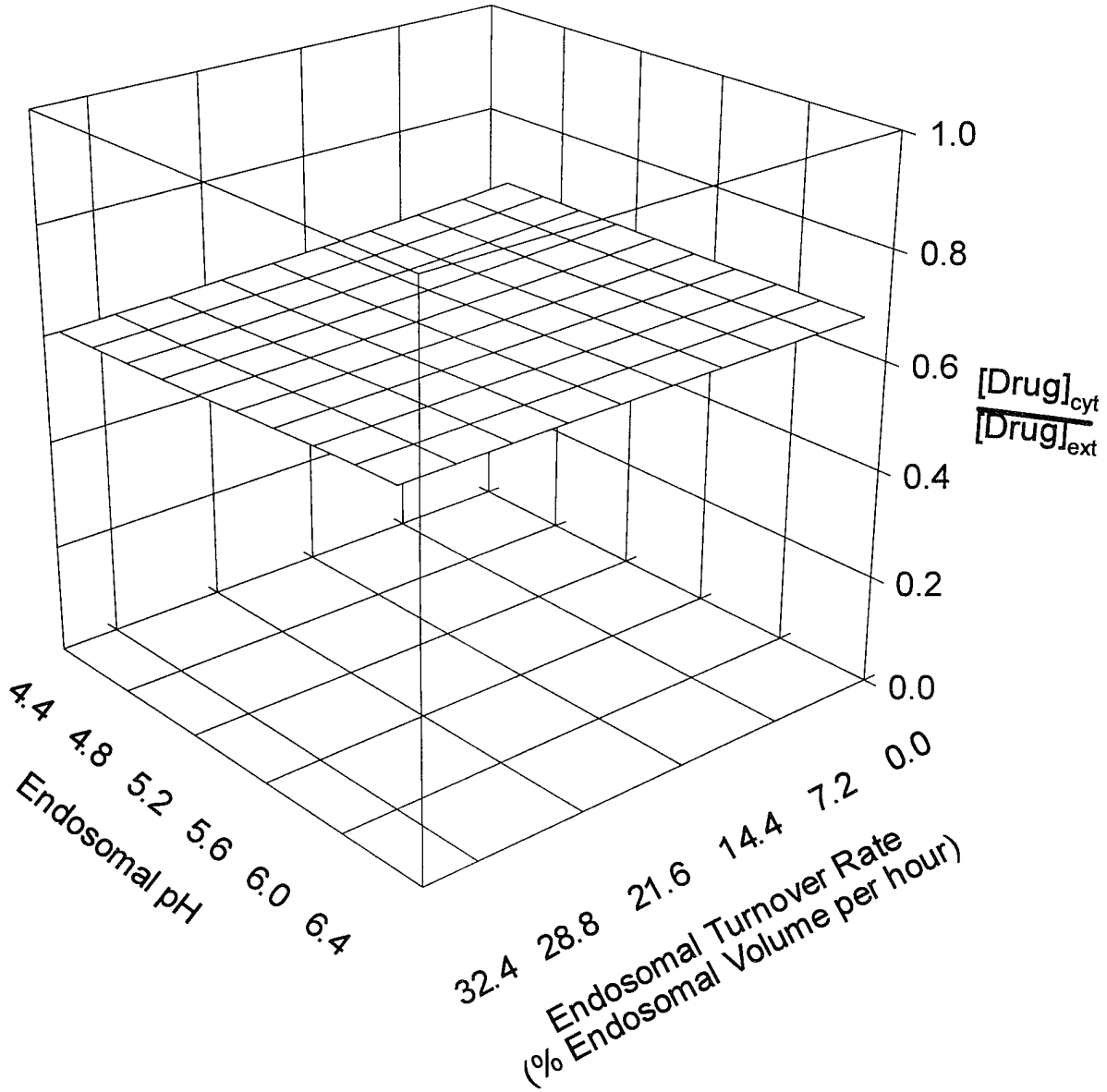

Figure 5

Drug pK_a = 9.0; $P_{DH,v}$ = 1x10^{-11} m/sec; $P_{DH,c}$ = 1x10^{-11} m/sec
k_H = 10$^{-7.5}$ M; V_T = 1.5x10^{-8} moles/(m^2-sec); k_{DH} = 150μM
Number of Endosomes = 200
Total Endosomal Volume = 1.0% of Cell Volume

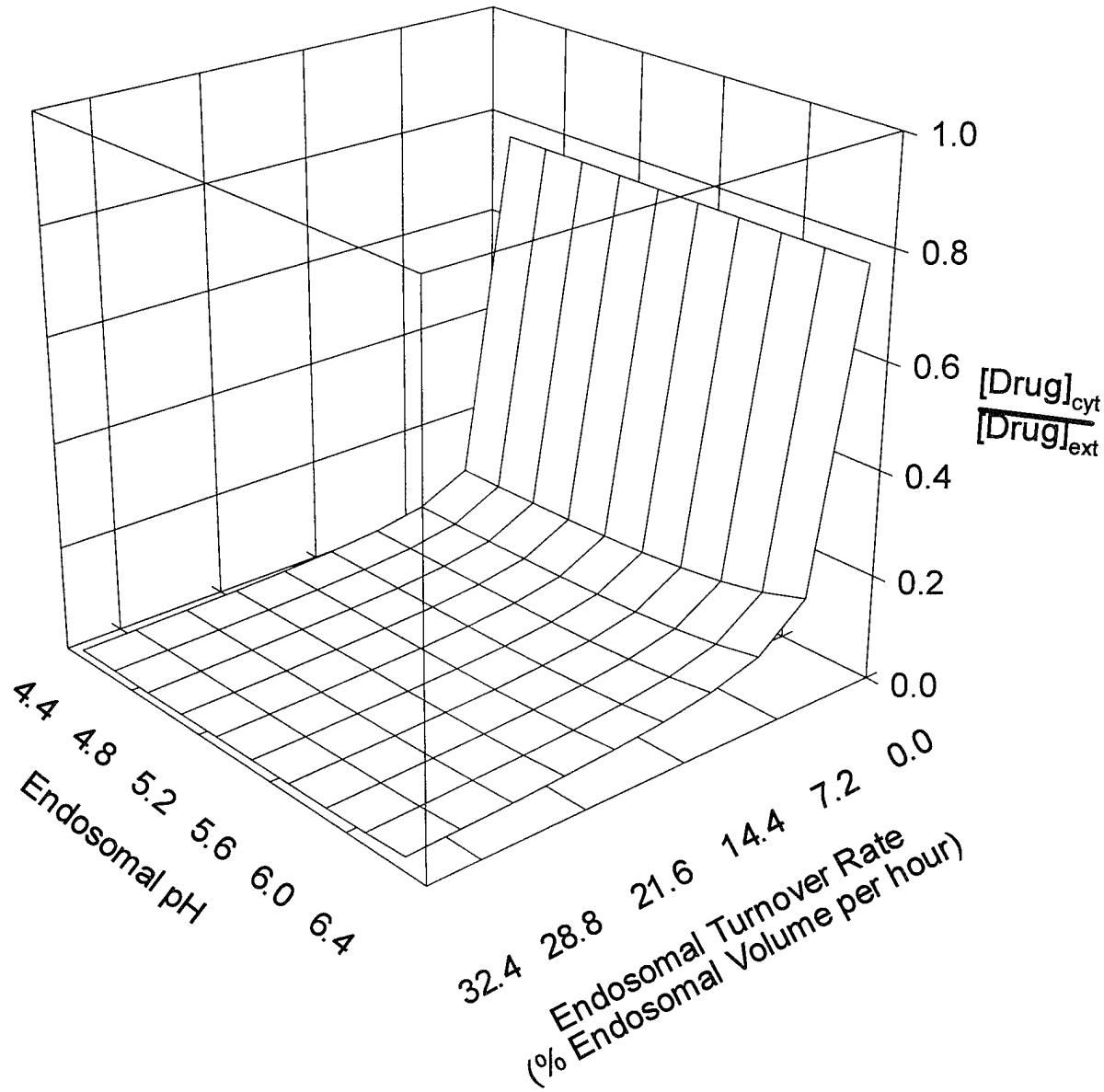

Figure 6

Drug pK_a = 9.0; $P_{DH,v}$ = 1x10^{-11} m/sec; $P_{DH,c}$ = 1x10^{-11} m/sec
k_H = 10$^{-7.5}$ M; V_T = 0.0x10^{-8} moles/(m^2-sec); k_{DH} = 150μM
Number of Endosomes = 200
Total Endosomal Volume = 1.0% of Cell Volume

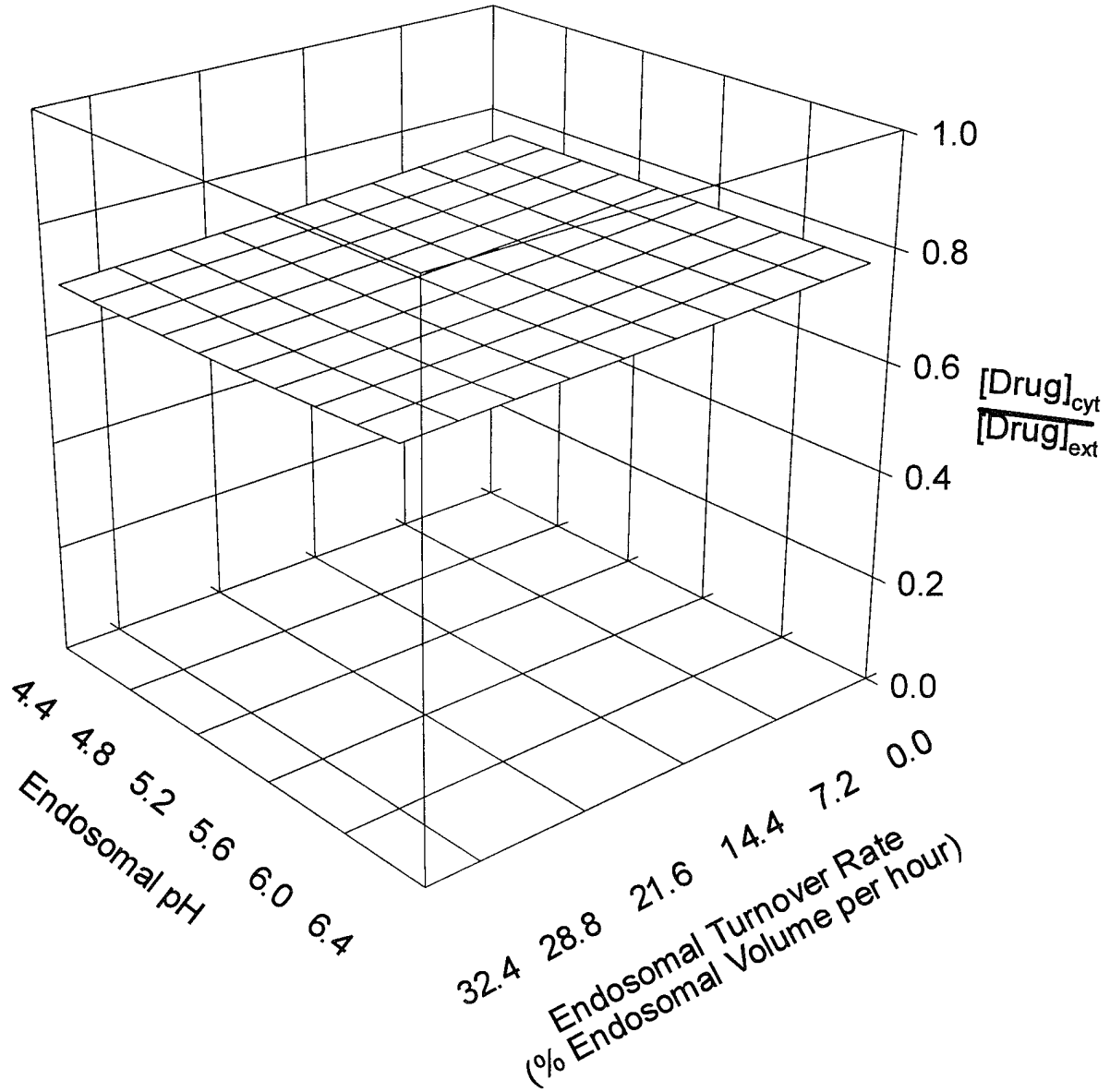

Figure 7

Drug pK_a = 9.0; $P_{DH,v}$ = 1x10^{-11} m/sec; $P_{DH,c}$ = 1x10^{-13} m/sec
k_H = 10$^{-7.5}$ M; V_T = 0.0x10^{-8} moles/(m^2-sec); k_{DH} = 150μM
Number of Endosomes = 200
Total Endosomal Volume = 1.0% of Cell Volume